MPLA based cationic liposome facilitates vaccine induced expansion of polyfunctional T cell immune responses against visceral leishmaniasis

Article *in* ACS Applied Bio Materials · September 2018

DOI: 10.1021/acsabm.8b00184

CITATIONS
11

READS
270

5 authors, including:

Amrita Das
Indian Institute of Chemical Biology
11 PUBLICATIONS **275** CITATIONS
SEE PROFILE

Mohammad Asad
Albert Einstein College of Medicine
59 PUBLICATIONS **248** CITATIONS
SEE PROFILE

Abdus Sabur
Raiganj Surendranath Mahavidyalaya
23 PUBLICATIONS **190** CITATIONS
SEE PROFILE

Nicky Didwania
Indian Institute of Chemical Biology
13 PUBLICATIONS **108** CITATIONS
SEE PROFILE

ACS APPLIED BIO MATERIALS

Article

MPLA based cationic liposome facilitates vaccine induced expansion of polyfunctional T cell immune responses against visceral leishmaniasis

Amrita Das, Mohammad Asad, Abdus Sabur, Nicky Didwania, and Nahid Ali

ACS Appl. Bio Mater., **Just Accepted Manuscript** • DOI: 10.1021/acsabm.8b00184 • Publication Date (Web): 11 Sep 2018

Just Accepted

ACS Publications

is published by the American Chemical Society. 1155 Sixteenth Street N.W., Washington, DC 20036

Title: MPLA based cationic liposome facilitates vaccine induced expansion of polyfunctional T cell immune responses against visceral leishmaniasis

Amrita Das, Mohammad Asad[#], Abdus Sabur, Nicky Didwania and Nahid Ali[*]

Affiliation: Infectious Diseases and Immunology Division,

CSIR-Indian Institute of Chemical Biology, 4, Raja S.C. Mullick Road, Jadavpur, Kolkata-700032, West Bengal, India.

∗ Corresponding author mailing address: Infectious Diseases and Immunology Division, CSIR- Indian Institute of Chemical Biology, 4 Raja S.C. Mullick Road, Jadavpur, Kolkata-700032. Telephone: 91 33- 24735197. Fax: 91 33 -24735197.

E-mail: nali@iicb.res.in.

Running Title: Liposomal DNA vaccination with MPLA against visceral leishmaniasis.

Abstract

Numerous experimental DNA vaccines have been tested against *Leishmania*, whose clinical use is mostly limited due to insufficient $CD8^+$ T cell-mediated immunity arising from poor gene delivery and/or presentation. Hence, there remains an important public health demand for a better vaccine adjuvant to combat leishmaniasis; ensuring proper antigen delivery coupled with strong cell mediated immune (CMI) response. To this end, we herein report, for the first time, novel cationic liposomes containing monophosphoryl lipid A (MPLA) intercalated into the 1,2-distearoyl-sn-glycero-3-phosphocholine (DSPC) lipid bilayer as an adjuvant for a DNA vaccine to enhance antileishmanial immunity. Interestingly, this MPLA-liposomal formulation strongly amplified the *Leishmania donovani* cysteine protease C (Ld*cpc*) DNA vaccine (i.e. pVAX1-*cpc*)-induced endogenous T cell and antibody responses with a Th1 biased profile. MPLA-liposomes could activate the splenic DCs *in vivo* and increased magnitude of antigen-specific polyfunctional $CD4^+$ and $CD8^+$ T cells together with $CD8^+$ IFN-γ^+ memory generation in BALB/c mice. Most importantly, I comparison to the mice receiving 'naked' pVAX1-*cpc*, immunization with MPLA-liposomal pVAX1-*cpc* DNA resulted in substantial reduction in parasite load, in association with reduced IL-10, IL-4 and TGF-β along with enhanced IFN-γ/IL-4 and IFN-γ/IL-10 cytokine ratios. Parasite burden inversely correlated with frequency of $CD4^+$ and $CD8^+$ T cells producing post-infection IFN-γ, IL-2 and TNF-α simultaneously, resulting in almost sterile protection (> 98%) conferred by the DNA vaccine entrapped in MPLA-liposomes. This DNA vaccine afforded potent central and effector memory cell formation, required for long-lasting immunity. Hence, this novel MPLA-DSPC adjuvant formulation approach could be a safe, biocompatible and amenable choice as a strong immunostimulating agent cum delivery system holding promise against leishmaniasis and several other infectious diseases in the near future.

Key words: Monophosphoryl lipid A, cysteine protease, visceral leishmaniasis, toll-like receptor, liposome, DNA vaccine.

1. Introduction

Visceral leishmaniasis (VL), also known as kala-azar, is a vector-borne deadly parasitic infection caused by *Leishmania donovani*/ *Leishmania infantum* accounting for nearly 200,000-400,000 new cases and death of about 40,000 people per year [1, 2] mainly belonging to poor socioeconomic background. To date, VL preventive strategies have limited themselves to vector and/or reservoir control, and treatment in endemic pockets. Antileishmanial treatment reportedly suffers from severe toxicity and chemoresistance [3]. This justifies an unmet medical need to develop a safe and efficient against leishmaniasis to eradicate this infection.

Although the lifelong immunity gained against reinfection marks the feasibility of a *Leishmania* vaccine, none has been successfully commercialized for human use. Global VL vaccine research has been pursued through variety of different yet complementary avenues, ranging from live or killed whole parasites to more defined recombinant protein/DNA based vaccines. Among these, genetic vaccination is considered as an attractive option[4]. In addition to the relative ease of production, safety and low cost, most importantly it allows stimulation of both major histocompatibilitycomplex (MHC) class-I and class-II antigen presentation to prime cytotoxic and helper T lymphocytes [5]. The multiantigenic DNA vaccine LEISHDNAVAX is currently under preclinical trials against both visceral as well as cutaneous forms of the disease [6, 7]. A few DNA vaccines for VL like Leishtec®, Leishmune® and CaniLeish® used for dogs have shown promising results[8]. However, despite the high molecular precision, limited immunogenicity of DNA vaccines in clinical trials has been the major deterrent factor for *Leishmania* vaccine due to lack of proper adjuvants [8, 9].

Most of the licensed vaccine adjuvants (like oil-in-water emulsion MF59 and aluminium salts) chiefly rely on humoral immunity without eliciting adequate cell mediated response. Immunity to the intracellular pathogens like *Leishmania*, however, requires both antigen-

specific $CD4^+$ and $CD8^+$ T cells for protection [10]. Conversely, progressive VL leads to T cell anerygy/exhaustion, thus facilitating parasite survival. In this regard, cationic liposomes have evolved as efficient delivery vehicles; promoting T cell based immunity as demonstrated in our recent studies [11, 12]. Despite variations in lipids, cationic surface charge of such liposomes interacts with negatively charged cell membrane to enhance the uptake of liposomal antigen [13]. Since naked DNA has a very short lifetime due to degradation by cellular nucleases, encapsulation within biodegradable nano- or microparticles like liposomes has tremendous benefits [14]. It ensures sustained release, better protection and increased phagocytosis of the antigenic biomolecules by professional antigen presenting cells (APCs), desirable for customized vaccine delivery. Cationic liposomes reportedly potentiate the plasmid DNA (pDNA) mediated innate immune activation by endosomal targeting, thereby increasing the TLR9 activation and efficient antigen presentation by the MHC class-I molecules[15, 16]. While liposomal delivery is capable of addressing the issues of poor antigen presentation and low bioavailability, it requires purposeful addition of a strong immunomodulator like MPLA to enhance the quality of CMI response in a human administrable route of vaccination [17, 18]. Monophosphoryl lipid A (MPLA), a disaccharide glycolipid, is a TLR4 ligand that has been clinically approved for human use as a safe vaccine adjuvant for hepatitis B (Fendrix®), HPV (Cervarix®) and melanoma (Melacine™) [19]. However, to our knowledge, there is no report of using MPLA containing liposomes as an adjuvant system for vaccination against *Leishmania*. Targeting a proper antigen is the most important criteria for vaccine success. Cysteine proteases form a major group of virulence factor in *Leishmania*. Leveraging on the limited success of rates of several protein and DNA vaccines in preclinical models [18, 20, 21], the present study aims to investigate the prophylactic potential of MPLA containing cationic DSPC liposomes as adjuvant with *L. donovani* cysteine protease type III (Ld*cpc*) (GenBank accession no. JX968801.1) DNA vaccine in the mice model of progressive VL. Leishmanial

cpc is a cathepsin B like protease encoded by a single-copy gene expressed throughout the life cycle of the parasite [22] that helps its survival inside host macrophages and disease onset [23, 24]. Furthermore, we demonstrated that *L. donovani* CPC is more protective compared to CPA/CPB, as a liposomal protein subunit vaccine against VL [18]. Although, we have used the MPLA-liposomal adjuvant platform for a DNA vaccine (pVAX1-*cpc*) against VL, this formulation is very attractive and versatile as a particulate delivery system. Remarkably, intramuscular immunization with pVAX1-*cpc* entrapped in this novel cationic MPLA-liposome resulted in robust vaccine-induced immunity against the fatal outcome of VL caused by *L. donovani*, which can be attributed to the dramatic expansion of multifunctional $CD4^+$ and $CD8^+$ T cells in the spleens of mice showing vaccine-induced protection. We also show that the MPLA-liposomal DNA vaccination leads to marked expansion of memory T cells (T_{CM}) after challenge infection, in addition to the short-lived effector T cells (T_{EM}), ideally required to combat intracellular pathogens like *Leishmania* and possibly cancers that rely on CMI response.

2. Materials and Methods

2.1. Animals and parasites

4-6 weeks old female BALB/c mice, reared under specific pathogen-free conditions in the animal care facility of the CSIR-Indian Institute of Chemical Biology were used for this study. All animal experiments were approved by the Committee for the purpose of Control and Supervision on Experimental Animals (CPCSEA), Ministry of Environment and Forest, Govt. of India, and the Animal Ethics Committee (147/1999/CPCSEA) of CSIR-Indian Institute of Chemical Biology. *L. donovani*, strain AG83 (ATCC® PRA413™), was maintained in Syrian golden hamsters [25]. The *L. donovani* promastigotes were cultured in Medium 199 (Sigma-Aldrich, St. Louis, MO) [11] and regularly sub-cultured to maintain an average density of 2×10^6 cells/ml.

2.2. Plasmid construction for DNA vaccine

The full-length *Ld*cpc gene from *L. donovani* (Gen Bank accession number JX968801.1) was cloned in frame into pVAX1 (Invitrogen, San Diego, CA) at the HindIII/BamHI restriction sites, using *Ld*cpc -specific primers and Pfx Taq DNA polymerase (Invitrogen) in a thermocycler (Gene Amp PCR System 9700; Applied Biosystems). PCR conditions were as follows: initial cycle of 94°C for 5 min, followed by 40 cycles of 94°C for 1 min, 58°C for 1 min 20 s, 72°C for 1 min 10s and a final cycle at 72°C for 7 min. The primers used were: 5′ CCC AAG CTT GGA ATG GGA GCC CTC CGC GCC AAG TCT 3′ (forward) and 5′ CGG GAT CC CTA CTC CTG CGC GGG TAT GCC AGC 3′ (reverse). Amplified PCR product was electrophoresced and eluted from gel (QIA quick gel extraction kit, Qiagen, Valencia, CA) for subsequent cloning into the mammalian expression vector pVAX1 (Invitrogen) and transformation into the competent *E. coli* TOP10 cells. The transformants were next screened for the presence of recombinant plasmid pVAX1-*cpc* [18]. The inserted gene was verified by

DNA sequencing (ABI Prism, Model 377; Applied Biosystems). Endotoxin-free pDNA was isolated using Endo-free plasmid isolation kit (Qiagen) according to the manufacturer's instructions to be used for all *in vivo* studies.

2.3. Transfection of plasmid constructs, reverse transcription-PCR and Western blot

The expression of *Ldcpc* gene was determined in mammalian cell by transfecting Human Embryonic Kidney-293 cells (HEK-293T) (ATCC®CRL-3216™, VA, USA) with pVAX1-*cpc* using Lipofectamine 2000 (Invitrogen), as detailed in Supplementary Materials and Methods. The cDNA synthesized from 100ng of total RNA using Superscript® III First-Strand Synthesis kit (Invitrogen, San Diego, CA) was amplified by PCR with *Ldcpc* -specific primers as mentioned in section 2.2. 10µl of each PCR product was subjected to 1% agarose denaturing gel electrophoresis (Tris-acetate buffer system, pH=8.2) and visualized by ethidium bromide staining. The pVAX1-transfected cells served as negative controls. For Western blot, the total protein extracted from transfected HEK-293T cells was subjected to SDS-PAGE, transferred onto a polyvinylidenefluoride (PVDF) membrane and incubated with a primary anti-rCPC polyclonal antibody (1:1000). The membrane was washed and probed with HRP- conjugated goat anti-rabbit IgG (1:1000) (Bangalore Genei, Bengaluru, India).

2.4. Preparation of MPLA-cationic liposomes and DNA entrapment

Cationic liposomes were prepared by dissolving 1, 2-Distearoyl-sn-glycero-3-phosphocholine (DSPC), cholesterol and stearylamine (SA) in a molar ratio of 7:2:2 using a previously described method [26], along with 10µg/ml MPLA (Invitrogen, San Diego, CA), in a glass bulb to form a thin film. After overnight desiccation, the lipid films containing DSPC-cholesterol-SA-MPLA and DSPC-cholesterol-SA were dispersed in 1 ml of 0.02M PBS (pH=7.4) with or without 1mg/ml of pVAX1-*cpc* DNA and incubated for 5 min at room temperature. The

mixture was then vortexed and sonicated twice in an ultrasonicator (Misonix, New York, USA) for 30s each, followed by 2h incubation at 4ºC. Unencapsulated free plasmid was separated by three successive ultracentrifugations (100, 000×*g* for 1h, at 4°C). Estimation of encapsulation efficacy values was based on DNA quantification in the unentrapped fraction by absorbance at 260 nm. The level of pDNA encapsulation in the cationic liposomes used ranged between 70-80%. The liposomes thus prepared, with or without pVAX1-*cpc* were stored at 4ºC until used. The loading content of MPLA in the liposomes was estimated using the chromogenic Limulus Amoebocyte Lysate (LAL) Assay kit (Lonza, Walkerville, MD) with the 1.5% of octyl β-D glucopyranoside (Sigma) detergent to solubilise the lipid bilayer [27], following manufacturer's protocol, which was approximately 100% (± 0.0015).

For green fluorescent liposomes, 0.1 mg/ml of Rhodamine 123 (Rh 123) (Sigma Life Sciences) was added in organic phase together with DSPC, cholesterol and stearylamine at a molar ratio of 7:2:2[18], along with 10μg/ml MPLA to form a lipid film. The unincorporated fluorochromes were separated by three successive washings in 0.02 M PBS by ultracentrifugation (100, 000×*g* for 1h, at 4°C).

2.5. Biophysical characterization of MPLA-liposomes

For atomic forced microscopy (AFM) imaging, 10μl of liposome samples were used, in acoustic alternative current mode, on Pico plus 5500ILM AFM (Agilent technologies, USA) Following a standard procedure described elsewhere [18], liposomal samples were deposited and dried for firm binding on freshly cleaved mica surfaces (ASTM V1 grade Ruby Mica, MICAFAB). Images were captured at 150-300 kHz oscillation frequency and finally processed and analyzed using Pico view (version 1.4) and Pico Image Advanced version softwares (Agilent Technologies).

For cryo electron microscopy (cryo-EM) 0.02M PBS containing MPLA- liposomes after 1:100 dilutions from stock solution were prepared following standard procedures with some modifications [28] and spread on cryo-EM grids. All the samples were observed using a Philips FEI (Eindhoven, Netherlands) Technai F20 field emission gun electron microscope under low-dose conditions using Oxford cryo-transfer holder at a magnification of 50,000×. The micrographs were recorded on 4K×4K CCD camera at a 15 μm (corresponding to 1.69 Å on object scale). 300 good images were selected among 500 total micrographs and subjected to automated 3D image reconstructions by Amira software package (Visage Imaging, Inc.) The particle size and zeta-potential of free and pDNA-loaded MPLA-liposomes were recorded by DLS (dynamic light scattering) on Zetasizer Nano-ZS (Malvern Instruments Corp, Workshire, UK). The liposome samples were diluted to the appropriate volume of double-filtered (0.22 μm pore size) distilled water. Particle size distribution was measured in terms of polydispersity index. For calculating encapsulation efficacy, pDNA content of the supernatants obtained after centrifugation of liposomes was subtracted from initial amount of DNA used during liposomal entrapment, using spectrophotometer (NanoDrop ND-1000, Thermo Fisher Scientific, USA). DNase I protection assay was performed following a standard protocol with slight modifications [29]. The samples tested were as follows: naked pVAX1-*cpc* and plasmid pVAX1-*cpc* entrapped in liposomal vesicles. A 1μg DNA aliquot of each sample was treated with 1μl DNase I (1U/μl) (Invitrogen, San Diego, CA), 1μl of 10X DNase I reaction buffer, and water to 10μl total volume and incubated at 37ºC for 15-60 min with constant rotation. The complexes were subsequently isolated using phenol-chloroform extraction, precipitated twice in the presence of ethanol and 3mM Na-acetate and resuspended in 30ml of TE buffer. Integrity of the pDNA was finally analyzed on 1% agarose gel electrophoresis with ethidium bromide staining.

2.6. Cell viability and *in vivo* toxicity

Freshly harvested peritoneal MΦs from healthy BALB/c mice were plated in 96-well microtiter plates (Nunc, Roskilde, Denmark) at a density of 10^6 cells/well with fresh RPMI 1640 with or without MPLA-liposomes (at concentrations 3.2-200 μg/ml with respect to DSPC), for another 1, 4 or 24h. MTT [3-(4,5-dimethylthiazol-2-yl)-2,5-diphenyltetrazolium bromide] assay was performed to determine the cell viability (supplementary Materials and Method). *In vitro* cell viability was evaluated in percent compared to untreated controls (taken as 100% viable).

In order to address the *in vivo* toxicity of MPLA-liposomal vaccine formulation, healthy 5-6 week old female BALB/c mice were divided into seven groups (n=7) and injected intravenously with MPLA-liposomes containing 50 μg or 100 μg plasmid DNA (with 1-2 mg of lipid w.r.t DSPC/animal/dose) in a 100μl injection volume in PBS, in a single, double or triple dose [30]. On day 15 after final injection, blood samples (300μl) were collected from tail vein of each animal and sera analyzed for levels of various toxicity markers: aspartate aminotransferase (AST or SGOT), alkaline phosphatase (ALP) and alanine aminotransferase (ALT or SGPT). All these hepatotoxicity parameters were determined spectrophotometrically for different groups using diagnostic kits following manufacturer's instructions (Randox, Ardmore, UK).

2.7. Liposome -mediated transfection, reporter gene assay and biodistribution of pVAX1- *cpc*

A day before transfection, RAW 264.7 cells were seeded in 24-well flat-bottomed cell culture plates (Nunc) at a density of 1×10^5 cells/well in 500μl of RPMI1640 medium without antibiotics until the cell number/well yielded 60-80% confluence the next day. After overnight incubation, cells were treated with the transfection mixture and MPLA-liposomes

with or without entrapped 0.8 μg pEGFP-N1 (Clontech) plasmid diluted in 25 μl OPTIMEM (Invitrogen) transfection medium and mixed by gently rocking the plates back and forth. RAW 264.7 cells were also transfected with pEGFP-N1mixed with Lipofectamine-2000 (Invitrogen), following manufacturer's protocol, taken as positive control. After another 6h incubation in a humified chamber (at 37ºC with 5% CO_2), 500μl of fresh RPMI was added to each well replacing the transfection medium. The cells were then washed with RPMI 1640 and returned to incubator for a further 18-24 h, prior to analysis to allow intracellular gene expression. Cells were finally visualized and photographed under an inverted fluorescence microscope (Nikon TS100) equipped with digital Nikon Coolpix 5000 camera, after 4% paraformadehyde fixation in 0.02ml PBS. For biodistribution study of our DNA vaccine in mice, isolation of genomic DNA was carried out using QIAamp genomic DNA isolation kit (Qiagen) from 20 mg of tissue samples: injection site (muscle), spleen, heart, liver and kidneys. Total gDNA were harvested after 48h following i.m. administration of 300μg of pVAX1- *cpc* entrapped in MPLA-liposomes. PCR assay was done on 100 ng of tissue gDNA with Ld*cpc*-specific primers and PCR conditions described previously and analyzed on 1% agarose gel with ethidium bromide staining. The gel picture was captured using Bio-Rad gel documentation system (Bio-Rad Laboratories, Inc., Hercules, CA).Tissue pDNA was quantified by densitometry compared to the known concentration of DNA using 1kb DNA ladder (Magspin-25) (APS Lab, Maharashtra, India).

2.8. Cellular uptake studies and antigen presentation

Cellular internalization study was conducted with fluorochromes Rh123 and Cy5 to observe the intracellular trafficking of MPLA-liposomes encapsulating pDNA. Murine peritoneal MΦs were incubated overnight in 0.5 ml of RPMI 1640 medium with 10% FCS, on glass coverslips (22mm^2, 10^6/coverslip). The plasmid pVAX1-*cpc* was labelled with Cy5 using FastTag® nucleic acid labelling kit (Vector laboratories Inc., Burlingame, CA). After

overnight desiccation, the Rh123-labelled lipid film was dispersed in 0.02 M PBS with or without Cy5-labelled pVAX1- *cpc* (700-1000 µg/ml) followed by three successive washings of fluorescent liposomes[18] in 0.02 M PBS to separate the excess free dye. Rh123 MPLA-liposomes containing Cy5-labelled pVAX1- *cpc* were added to adherent MΦs, followed by 2h incubation at 37º C. After 4% paraformaldehyde (Sigma- Aldrich) fixation, the cells were mounted onto glass slides with Prolong Gold containing DAPI (Invitrogen). Additionally, to track intracellular docking of labelled liposomes inside MΦ at 2 h, cells were incubated with LysoTracker Red (Molecular Probes, Eugene, Oregon). Fluorescence signals were observed under Andor Spinning Disk Live Cell Confocal microscope (Andor Technology Plc., Belfast, Ireland) equipped with a 60× objective (Olympus), Andor iXon3897 EMCCD camera and Andor iQ Live Cell Imaging software. DAPI, Rh123 and Cy5 were excited with a 405-nm, 488-nm and 577-nm argon laser, respectively. Adobe Photoshop (CS3, Adobe Systems) software was used to arrange the final images.

To have a quantitative insight into uptake efficacy, cellular uptake of cationic Rh123 labelled liposomes were also studied by flowcytometry. RAW 264.7, MOLT-4, C6, K562, HCT116 and U937 cell lines were cultured using RPMI1640 or DMEM/10% FCS (37 ºC, 5% CO_2). Cells were routinely seeded in 75 cm^2 cell culture flasks (Costar) at a density of 2×10^6 cells, splitting after every 2 days. Cells were incubated with medium containing Rh123 labelled liposomes (50mM w.r.t DSPC) in serum-free RPMI 1640 for designated time points. Following cell detachment using trypsin/EDTA and washing, cells were fixed and permeabilized with Cytofix/Cytoperm (BD Biosciences) and finally analyzed on FACS LSR Fortessa Flowcytometer (Becton Dickinson) using FACS Diva software (BD Biosciences), for liposomal uptake. To assess the antigen presentation pathways used by the cationic liposomes with or without MPLA, bone-marrow derived dendritic cells (BMDCs) generated from BALB/c mice were subsequently stimulated with free cationic liposomes with or

without intralamellar MPLA at a specific concentration (supplementary Materials and methods). After 18 h of incubation in RPMI 1640/10% FCS (at 37°C, 5% CO_2) the cells were subjected to western blots with antibodies to Gilt (T-18), Calregulin (T-19), TAP-1(M-18), Tapasin (H-15), Cathepsin-S (M-19), Cathepsin-H (N-18) (Santacruz Biotechnology Inc., Dallass, TX) and β-actin (Sigma). The blots were then incubated with HRP-conjugated secondary antibodies (Sigma) followed by final washing and development of the PVDF membranes (Millipore) using enhanced chemiluminescence (ChemiDoc MP Imaging system, Bio-Rad).

2.9. Immunization and challenge infection

For immunization studies, a total of 84 healthy, 4-6 weeks old female BALB/c mice were divided into following six groups, each containing 14 animals as described below: group 1, unvaccinated (PBS controls); group 2, empty liposome (without MPLA) vaccinated (CL); group 3, empty MPLA-liposome vaccinated [CL(MPL)]; group 4, naked pVAX1-*cpc* vaccinated (pVAX1-*cpc*); group 5, liposomal DNA vaccine without MPLA [pVAX1-*cpc*/CL]; group 6, MPLA-liposomal DNA vaccine [pVAX1-*cpc*/CL(MPL)]. The experimental schedules for immunization were conducted as follows:

Day 0: immunization. Mice of group 4 were immunized with 50 μg of naked pVAX1-cpc in 50 μl of PBS, i.m. in the thigh muscle of the hind leg, group 5 was immunized i.m with 50 μg of pVAX1-*cpc* entrapped in liposomes (without MPLA) in 50 μl of PBS, whereas group 6 was immunized i.m with 50 μg of pVAX1-*cpc* entrapped in MPLA-liposomes in 50 μl of PBS. Groups 2 and 3 serves as adjuvant controls, being injected with empty liposomes (without MPLA) and MPLA-liposomes diluted in PBS, respectively.

Day 14: after immunization. All groups received one boost dose of DNA vaccine or adjuvants i.m. similar to the first immunization.

Day 16: after immunization. Four mice per group were sacrificed for assessment of DC stimulation in vivo.

Day 22: after immunization. Five mice per group were taken out for collection of blood, peritoneal MΦs and finally sacrificed for immunological assessment of cellular responses.

Day 24: after immunization. Remaining animals from all groups were challenged with 2.5 × 10^7 freshly transformed stationary phase promastigotes of *L. donovani* intravenously, in 200 µl of 0.02 M PBS as described earlier [30]. Three months after infection (day 114 after immunization), experimental animals (n=5) were sacrificed for immunological and parasitological assessment of disease progression.

2.10. Delayed type hypersensitivity (DTH)

DTH response was recorded, ten days after final immunization, as a predictor of CMI response. For calculating DTH, the difference in footpad swelling (in mm) of the test footpad (injected with 50µl of 5µg/ml endotoxin-free rCPC) from the control footpad (injected with 50µl of 0.02 M PBS) was determined after 24h of intradermal injection using a constant pressure calliper (Starret, Anthol, USA) [25].

2.11. rCPC specific humoral response

To determine the antibody responses, enzyme-linked immunoglobulin assay (ELISA) [25] was performed using serum samples collected from each experimental animal per group to analyze the rCPC-specific immunoglobulins before and after infection. Briefly, In brief, 100 µl of rCPC (50µg/ml) diluted in 0.02M PBS was coated on 96-well microtiter plates (Nunc, Naperville, IL) and incubated at 4ºC overnight. To prevent non-specific binding, the plates were then blocked, washed and finally incubated with mice sera at 1:200 dilution, followed by 1:5000 diluted horseradish-conjugated goat anti-mouse IgG (Sigma-Aldrich), IgG2a and

IgG1 (1:1000 dilution) (BD Pharmingen, San Diego, CA). After developing the coloured reaction, the absorbance data was recorded at 450 nm in an ELISA plate reader (Thermo, Waltham, MA).

2.12. In vitro antileishmanial activity, assessment of nitric oxide (NO) and reactive oxygen species (ROS)

Peritoneal MΦs collected from differently immunized BALB/c mice were allowed to adhere to 18 mm^2 glass coverslips (10^6 MΦ/coverslip) in 500µl of RPMI 1640/10% FBS. After overnight incubation at 37 ºC with 5% CO_2, MΦs were infected *in vitro* with virulent *L. donovani* promastigotes following an optimized protocol [18]. 72 h post-infection, culture supernatants were obtained and kept frozen at -70 ºC for estimation of nitric oxide (NO), and the cells were then fixed in methanol and Giemsa stained for determining number of intracellular parasites. MΦs culture supernatants were subsequently analyzed for NO (expressed as µM nitrite) using Griess reagent [31].

The generation of intracellular reactive oxygen species (ROS) by the peritoneal MΦs was determined using the oxidant sensitive non-fluorescent dye 2', 7'-dihydrodichlorofluorescin diacetate (H_2DCFDA) (Molecular probes) which gets converted into green fluorescent dye dichlorofluorescein (DCF) in the presence of free radicals [32]. Briefly, infected peritoneal MΦs from different groups were stained with 10µM H_2DCFDA for 30 min in serum-free medium. After removal of excess free dye by washing twice with fresh RPMI 1640 and a final wash in 0.02 M PBS, fluorescent signals were obtained using a microplate reader (Synergy H1, BioTek; Excitation: 485nm; Emission: 528 nm) and expressed as percent of control.

2.13. Cytokine ELISA

For determination of rCPC specific total cytokine production, 10 days after last immunizations, spleens were removed aseptically from the differently immunized animals and prepared into single cell suspensions by teasing between 20μm pore-size sieve [11]. Briefly, splenocytes (2×10^5 cells/well) were plated in 96-well flat-bottomed tissue culture plates (Nunc) in 200 μl volume, for 72h (at 37ºC, 5% CO_2), with or without stimulation with rCPC (2.5μg/ml). Interleukin (IL)-4, IL-12, IL-10 and IL-2 concentrations were quantified in the culture supernatants using OptEIA ELISA kits (BD Pharmingen) as detailed earlier [11].

2.14. Cell proliferation assay

Spleens were aseptically removed from immunized animals 3 months post-infection and single cell suspensions were prepared [11]. The spleen cells were labelled with carboxyfluorescein succinimidyl ester (CFSE) (Molecular Probes), according to the standard procedure [11, 32] with slight modifications. Briefly, 1×10^7 splenocytes/ml was incubated for 10 min at 37 °C with CFSE (2μM). Quenching of CFSE dye was carried out by addition of one volume of cold 0.02 M PBS followed by washing with cold RPMI 1640. Cells (1×10^7 cells/ml) were cultured for 5 days in 24-well flat bottomed tissue culture plate (Nunc) in triplicate after stimulation with rCPC (2.5μg/ml) or conA (2.5μg/ml) [11]. 5 days post-incubation, cells were collected, washed and labelled with PE conjugated anti-CD3, PerCP Cy5.5 conjugated anti-CD-4 and APCCy7 conjugated anti-CD8 mAb at 4°C for 30 min. The percentage of proliferating $CD4^+$ and $CD8^+$ T cells, i.e. CFSE ^{low} cells was determined from the gated $CD3^+$ cell population using FACSCanto flowcytometer (Becton Dickinson) and analysed by the FlowJo software version 10 (TreeStar Inc., OH, USA).

2.15. Assays for antigen-specific immune T cells and DCs

Staining of intracellular cytokines IL-12, IFN-γ, IL-2, IL-4, IL-10 and TNF-α was carried out following a previously published protocol [11] with slight modifications. Briefly, single-cell suspensions of spleen cells from the experimental animals were stimulated overnight with or without 2.5μg/ml rCPC. 2h after addition of Brefeldin A (10mg/ml), cells were harvested and washed in 0.02 M PBS containing 0.1% NaN_3 and 1% FCS [11]. Cells were stained with fluorochrome labelled monoclonal antibodies (all purchased from BD Pharmingen): PE conjugated anti-CD3, APCCy7 conjugated anti-CD8 and PerCP Cy5.5 conjugated anti-CD4 mAb for 30 min at 4°C. After permeabilization, the cells were next stained with fluorochrome labelled anti-mouse IFN- γ, IL-2, TNF-α, IL-10, 1L-4, CD44, and CD62L mAbs. The cells were incubated in the dark for 30 min at 4°C. After final washing in wash buffer, the cells were resuspended in 0.02 M PBS. Within 24h, samples were read on an LSR Fortessa flow cytometer, using FACSDiva software (BD Biosciences). Flowcytometric data were analysed by FlowJo software version 10 and Boolean gating was applied to determine the functional categories of both $CD4^+$ and $CD8^+$ T cells.

In another set of experiment, four mice were i.m. immunized with 50 μg of pDNA entrapped in cationic DSPC liposomes formulated with or without MPLA, designated as: pVAX1-*cpc*/CL (MPL) and pVAX1-*cpc*/CL respectively, naked pVAX1-*cpc*, empty DSPC liposomes with or without MPLA, designated as: CL (MPL) and CL respectively or PBS. 48h post-immunization, animals were sacrificed, spleens were removed and single cell suspensions of spleen cells from individual animals were prepared. Plasmacytoid DCs were separated using magnetic-activated cells sorting columns (MACS) and mouse plasmacytoid DC isolation kit II (Miltenyi Biotec, Auburn, CA), following the manufacturer's protocol. To quantify the surface expression of costimulatory molecules, splenic DCs (1×10^6 /sample) from differentially vaccinated mice were incubated with fluorochrome conjugated anti-mouse CD11c, B220, MHC-II, CD80, CD86 and CD40 antibodies in dark for 30 min at 4ºC.

Finally, the isolated DCs were washed thrice with 0.02M PBS containing 0.5% BSA and 0.1% NaN_3 (FACS buffer), resuspended in 0.02M PBS and subjected to FACS analysis using LSR Fortessa (BD Biosciences).

2.16. Evaluation of parasite burden

The efficacy of naked and liposome-encapsulated pVAX1-*cpc* plasmids to protect animals against lethal *L. donovani* challenge, by intramuscular immunization, was evaluated in murine model of progressive VL. After 3 months of challenge infection, organ parasite load was expressed as Leishman-Donovan units (LDU) [34] by microscopic examination of the Giemsa-stained impression smears of liver and spleen samples from experimental groups. LDU was calculated by the following formula: number of amastigotes/ 1000 cell nuclei × organ weight (in mg) [34, 59].

Further, parasite load was also determined by a more sensitive Limiting Dilution Assay (LDA), as detailed by Titus et al. [35] Briefly, infected liver and spleens were aseptically removed from the experimental animals and homogenized in Schneider's Insect medium (Sigma)/10% FCS, penicillin (100U/ml) and streptomycin (100mg/ml). Homogenates were serially diluted (five-fold) and cultured in 96-well tissue culture plates (Nunc) at 21°C for 3 weeks for the presence of viable parasites [11, 18.] The total organ parasite burden was determined from the respective organ weights following a standard procedure [11, 35].

2.17. Statistical analysis

One-way analysis of variance (ANOVA) with Tukey-Kramer post-test was performed to compare the differences between multiple groups. Two-sample data were compared using Student's t-test for assessing the statistical significance. Statistical calculations were performed using the Graphpad Prism 5.0 (http://www.graphpad.com). A p value < 0.05 was considered significant for all analyses.

3. Results

3.1. DNA vaccine pVAX1-*cpc* construction and its expression in mammalian cell line

Full-length cysteine protease C gene of *L. donovani* AG83 (ATCC PRA-413) (Ld*cpc*) was cloned in the eukaryotic expression vector pVAX1 (Fig. 1A) and referred to as pVAX1-*cpc*. The positive clones selected by restriction digestion were reconfirmed by sequence analysis (Fig. 1B). Transcription of Ld*cpc* at the mRNA and protein levels from pVAX1-*cpc* in transfected HEK- 293T cells was checked by reverse-transcription PCR (RT-PCR) (Fig.1C) and immunoblot analysis (Fig. 1D) using anti-rCPC antibody, respectively. These results depict a 1.038 kb band in RT-PCR (Fig.1C) which confirms correct construction and of the recombinant and its successful expression in mammalian cell line. Blank vector- transfected HEK-293T cells showed no band in western blot (Fig.1D). For production of recombinant rCPC, the overexpressed rCPC produced by *E. coli* BL21 (DE3) harbouring pET28a-Ld*cpc* was subjected to His-tag purification through Ni^{2+}-NTA column [22]. The expression status of the cloned gene at protein level showed the purified rCPC protein to be essentially homogeneous (Fig.1E)

3.2. Biophysical characterization of MPLA-liposomes

The particle size, distribution and charge are important factors governing cellular internalization and their ability for slow release of entrapped biomolecules [36]. The AFM images of the cationic liposomes in the acoustic alternative current (AAC) mode with and without entrapped plasmid, on mica are shown in Fig. 2A-D. Flattening of vesicles on the mica support just few minutes after deposition indicates a moderate stability of the liposomes on a mica substrate. Two-dimensional and three-dimensional AFM images further revealed the smooth, spherical and well-defined structure of liposomes with very few aggregations. The mean hydrodynamic diameter of empty DSPC liposomes containing MPLA i.e. CL

(MPL) was 151 ± 23.86 nm as determined by Zetasizer Nano-ZS (Malvern Instruments), with a zeta potential of 24.3 ± 3.1 mV, indicating a net cationic charge at pH 7.4 (Table 1). The entrapment of pDNA pVAX1-*cpc,* denoted as pVAX1- *cpc*/CL (MPL), slightly reduced the size and positive charge of vesicles to 134 ± 14.31 nm and 22.6 ± 1.2 mV respectively. The polydispersity index of empty (0.52 ± 0.25) and plasmid entrapped (0.66 ± 0.31) liposomes show the heterogeneity in particle size of the formulations. The level of DNA incorporation ranged between 70–80%. The zeta-potential values of the liposomes usually indicates the total surface charge on the vesicles and hence can be used to predict the extent of interaction between the positive charge of the lipid bilayer and the negatively charged DNA [14,15]. The cationic liposomes make a strong association with the anionic phosphate backbone of the DNA molecute [14, 37]. Hence, entrapment of plasmid DNA into cationic liposomes probably led to neutralization of some positive charges and compaction leading to decrease in the zeta potential and size of the liposomes studied (Table 1). Also, intercalation of MPLA molecules in phospholipid bilayer of cationic liposomes may lead to a more negative zeta potential as reported earlier [38, 39].

Fig. 2E and F show cryo-TEM micrographs of MPLA-liposome preparations and their 3D reconstruction, respectively, at low concentrations. Empty MPLA-liposomes show clearly smooth and spherical vesicles with mean diameter 150-170 nm. The structures were well maintained after pDNA entrapment (data not shown) which show slightly rippled texture with bulges possibly caused by associated DNA. Furthermore, our results of AFM and cryo-TEM examinations were in good correlation with the results of DLS analysis. Overall, the size and surface charge of these liposomes (with or without MPLA) are ideal for sterile filtration, uptake by APCs [40, 41] and a better lymph node targeting (supplementary Fig. S6), consistent with previous reports [42].

3.3. Transfection efficacy, cellular uptake and stability of MPLA-liposomes

We next investigated the gene delivery functions of MPLA-liposomes on different cell types, especially those that closely resemble target cells. In the current work, transfection of RAW 264.7 MΦ cell line with pEGFP-N1 was carried out under similar conditions to evaluate the transfection efficacies of cationic MPLA-liposomes and Lipofectamine 2000. Untreated RAW 264.7 cells were taken as controls. Plasmid DNA encapsulated in cationic liposomes (without Ca^{2+}) was capable of transfecting the RAW 264.7 cell line (Supplementary Fig.S1, A) as detected by GFP expression observed under fluorescent microscope. Under identical concentrations of DNA (200 ng), MPLA-liposomes resulted in fluorescence comparable to that of Lipofectamine 2000 (taken as positive controls) complexed plasmid (Supplementary Fig.S1, A). Quantitative determination by flowcytometry further revealed upto 4-fold higher uptake of MPLA-liposome entrapped pEGFP-N1 in comparison with free pEGFP-N1 following 6h of incubation (Supplementary Fig.S1, B). As expected, naked plasmid pEGFP-N1 by itself has limited capacity of transfection.

For visual confirmation of liposomal DNA entry into the cells, fixed-cell confocal laser scanning microscopy (CLSM) studies were carried out with mouse peritoneal MΦs, that allow for the tracking of fluorescent labeled pDNA (pVAX1-*cpc*) within liposomes as it enters and traverses the intracellular environment. Cy5 (red) labeled pVAX1-*cpc* was encapsulated in Rh123 (green) labeled DSPC liposomes consisting of intrabilayer MPLA, and added to the culture of peritoneal MΦs as detailed in Materials and Methods. Most of liposome encapsulated pVAX1-*cpc* pDNA was delivered efficiently into MΦs, as indicated by colocalization (yellow color) of the green and the red signals from Rh123 labeled MPLA-liposomes and Cy5 labeled pDNA respectively (Fig. 3A and supplementary Fig. S2, A). Interestingly, CLSM analysis also revealed an increased uptake of Rh123 MPLA-liposomes

containing pDNA in *L. donovani* infected MΦs compared to uninfected normal MΦs (Fig. 3A and supplementary Fig. S2, A), after an hour of incubation. This augmented liposomal uptake in *Leishmania* infected MΦs was probably due to disruption membrane lipids, increased membrane fluidity [43] and phagocytic behaviour of MΦs after infection [44]. Our results show that DNA vaccine entrapped in liposomes is also effective against *Leishmania*-infected MΦs, which indicates the possible therapeutic success of our MPLA-liposomal DNA vaccine formulation against *Leishmania*. Quantitative evaluation of cellular uptake of these MPLA-liposomes was also evaluated using flowcytometry (FACS) in peritoneal MΦs (Fig. 3B and C) and different cancer cell lines (supplementary Fig. 2B). Results showed robust intracellular uptake of the Rh123 MPLA-liposomes in all the cell lines with little differences, possibly due to different behaviors of these cell lines. In general, internalization of liposomes was higher at 2-3 h, expressed by higher mean fluorescence intensity (MFI) which subsequently diminished after 4 h of incubation (Fig. 3C). The results support our interpretation that cellular uptake of MPLA-liposomes occurs in a time-dependent manner and which follows its intracellular fate of antigen release at higher time points. Rh123 MPLA-liposomes also facilitated successful lymph node entry as observed after i.m. administration in BALB/c mice (Supplementary Fig. S6), which shows their potency as good delivery vehicles for vaccines.

To elucidate the antigen presentation pathways used by liposomal processing of exogenous antigens, BMDCs were stimulated with cationic liposomes formulated with or without MPLA. As shown in Fig. 3D, stimulated BMDCs strongly expressed the MHC Class-I (TAP1, tapasin, calregulin) associated molecules which was further augmented by MPLA-liposomes, and also MHC class-II (GILT, cathepsin H and cathepsin D) associated molecules. This result of this MHC associated protein expression profile is consistent with

the fact that this liposomal vaccine formulation can stimulate both $CD4^+$ and $CD8^+$ T cell response towards entrapped antigen (Fig. 8) in experimental mice.

Next, the extent of protection conferred by liposomal entrapment against nuclease degradation was studied using the model enzyme DNAse I. Fig. 4A, clearly demonstrate that most of the pDNA incorporated inside the cationic liposomes [pVAX1-*cpc*/CL (MPL)] could not be degraded by DNAse I. In contrast, naked plasmid pVAX1-*cpc* was degraded within 15 minutes upon exposure to the enzyme. This may result from the condensed state of pDNA encapsulated within the cationic liposomes which is resistant to DNAse action [45]. Results were largely confirmed by agarose gel electrophoresis of samples exposed to DNase I (Fig. 4A). Based on intensity of staining and the appearance of smearing, it can be seen that, whereas naked plasmid DNA was completely digested (Fig. 4A, lanes 2 and 3), DNA entrapped in cationic liposomes under study was fully protected as observed with (Fig. 4A, lane 4) or without (Fig. 4A, lane 5) phenol: chloroform extraction. Most of the DNA was entrapped in the liposomes and retarded in the gel as no free DNA is seen in lane 5. Hence, the pDNA encapsulated in the MPLA-liposomes shows increased stability compared to naked plasmid against degradation before entering the cells, maximizing the benefits of genetic vaccination.

3.4. MPLA-liposomes are well tolerated and potentially non-toxic for successful DNA delivery

To ascertain the biocompatibility of the liposomal formulation and absence of cytotoxicity, both dose and time-dependent MTT assays were carried out by exposing the normal mouse peritoneal MΦs to graded concentrations of MPLA-liposomes over a 1h-, 4h- and 12h- time period (Fig. 4B). It is worth noting that at all examined time points, none of the concentrations of MPLA-liposomes had any significant effect on cell viability of MΦs. Even

at very high liposome concentrations between 100-200 μg/ml there was negligible reduction of the viability by 10-15% after 4 h of incubation, which remained almost constant thereafter, indicating that the liposomal formulation is non-toxic, biocompatible and totally safe for *in vivo* use.

Next, we studied the relative *in vivo* toxicity of the vaccine formulation containing pVAX1-*cpc* entrapped in MPLA-liposomes, in BALB/c mice to confirm our *in vitro* results. The hepatotoxicity, if any, following administration of liposomal vaccine was monitored by evaluating the levels of ALT, AST and ALP, in the serum of DNA-injected and normal mice, following 14 days post immunization via intravenous (i.v.) route (Fig. 4, C-E). ALT is a hepatocyte protein which primarily increases in liver damage. AST is found in most tissues but predominantly present in liver, cardiac and skeletal muscles. High AST level is an indication of systemic tissue damage, especially liver dysfunction. ALP is present in all the tissues throughout the body with highest concentrations in biliary tract, liver and bones. Increase in serum ALP level, a normal excretory product in bile, reflects liver injury due to toxins. Our results indicated that, administration of more than 50μg of liposomal pDNA/animal showed minor increase of AST level compared to controls (Fig.4C). However, these differences remained statistically insignificant, indicating no aberrant liver function in mice after immunization. ALT and ALP levels (Fig.4, D and E respectively) remained almost within normal limits for all the immunization doses, compared to controls.

Biodistribution studies of pVAX1-*cpc* entrapped in MPLA-liposomes by conventional PCR and densitometry (Supplementary Fig. S7) analysis shows presence pDNA copies in all the tissues, maximum concentration (78.05 ± 20.3 ng/20 mg) being detected in muscles of hind leg (injection site), followed by spleen (35.11 ± 13.3 ng/20 mg), heart (29.14 ± 6 ng/20 mg),

liver (14 ± 5.5 ng/20 mg) and kidneys (12 ± 14.2 ng/20 mg), at 48 h post-injection. No PCR reaction product could be detected in controls (vector-injected).

3.5. Comparative anti-leishmanial activities of liposomal pVAX1-*cpc* with or without MPLA

Given the significant role of mammalian MΦs in innate immunity and multiplication of *Leishmania* parasites, we monitored the anti-leishmanial efficacy of our liposomal DNA vaccine *in vitro* using murine peritoneal MΦs. Resident peritoneal MΦs obtained from peritoneum of immunized BALB/c mice were incubated for 72h after initial *in vitro* infection with virulent *L. donovani* promastigotes for 4h. While the mean number of amastigotes/MΦ increased with time i.e. 24-72 h in PBS or adjuvant controls, parasite multiplication was markedly suppressed in liposomal pVAX1-*cpc* immunized groups. Further, the number of amastigotes in the infected MΦs from mice immunized with MPLA-liposomal pVAX1-*cpc* was significantly lower (Fig. 4G) in comparison to the liposomal pVAX1-*cpc* without MPLA ($p < 0.05$); suggesting that incorporation of MPLA in liposomal vaccine formulation contributes to maximum MΦ stimulation to stop parasite multiplication. Partial anti-leishmanial effect was also observed in MΦs from naked pVAX1-*cpc* immunized mice at 72 h, suggesting the vaccine potency of Ld*cpc* alone. Since NO and ROS from stimulated MΦs are crucial for the killing of intracellular *Leishmania* [46, 47], we investigated their production in cell free culture supernatants from infected MΦs from immunized mice. Interestingly, after 72h of *in vitro* infection, MΦs from MPLA-liposomal pVAX1-*cpc* immunized animals released highest amounts of NO and ROS which were respectively ~2 fold and 1.6 fold ($p < 0.001$) higher than the naked pVAX1-*cpc* immunized animals after 72 h post culture (Fig. 4H and I). Altogether, our results indicated that the DNA vaccine formulation in presence of MPLA [i.e. pVAX1-*cpc*/CL(MPL)] showed highest action

towards *Leishmania* elimination from infected MΦs compared to DNA vaccine alone (i.e. pVAX1-*cpc*) or DNA vaccine entrapped in liposomes without MPLA [i.e. pVAX1-*cpc*/CL]. Protection against *L. donovani* infection can clearly be associated with induction of oxidative burst in MΦs, which in turn favours the host innate immunity and corroborate intracellular parasite killing.

3.6. MPLA-liposomal DNA vaccine stimulates strong DTH and Ag-specific CMI response *in vivo*

Suppression of CMI response is a hallmark of active VL both in animals and human [48, 49]. Therefore, to address whether the liposomal DNA vaccination can restore the protective cellular immunity *L. donovani* challenged mice, we performed DTH and lymphocyte proliferation assay for different vaccinated groups, 3 months post-infection. Immunization of mice with pVAX1-*cpc* alone, in association with cationic liposomes, with or without MPLA, all increased the DTH response significantly in BALB/c mice (Fig. 4J, $p < 0.05$) in comparison to PBS. The highest DTH response correlated well with the protection in pVAX1-*cpc*/CL (MPL) immunized mice, which was also significantly higher than naked pVAX1-*cpc* and pVAX1-*cpc*/CL immunized groups ($p < 0.0001$). Among the different vaccinated groups, the adjuvant controls exhibited comparable levels of DTH, whereas DTH was significantly increased in naked pVAX1-*cpc* immunized group ($p < 0.05$), both before and after *L. donovani* infection. Virulent *L. donovani* challenge further elevated DTH responses in all vaccinated groups (supplementary Fig.S5). Mice receiving pVAX1-*cpc* entrapped in MPLA-liposomes exhibited the highest degree of DTH which was statistically significant over the mice receiving pVAX1-*cpc* alone ($p < 0.001$) or pVAX1-*cpc* entrapped in cationic liposomes without MPLA ($p < 0.0001$) (supplementary Fig.S5).

Similarly, lymphoproliferation assay also revealed the restoration of cellular immunity after *L. donovani* challenge in liposomal DNA vaccinated mice. As shown in Fig. 5A and B, conA (taken as positive control), highly enhanced both $CD3^+CD4^+$ and $CD3^+CD8^+$ T cell proliferations *in vitro*, as assessed using CFSE. The gated $CD3^+CD4^+$ and $CD3^+CD8^+$ T cells from all the DNA immunized animals proliferated upon antigenic restimulation, the response being significantly higher for both cell types ($p < 0.05$ and $p < 0.001$ respectively) in pVAX1-*cpc*/CL (MPL) immunized animals, compared to infected controls. Liposomal pVAX1-*cpc* vaccination with MPLA induced highest T cell proliferation, the $CD3^+CD8^+$ T cell proliferation being significantly higher ($p < 0.05$) than $CD3^+CD4^+$ T cells in this group. The percent proliferation of $CD3^+CD8^+$ T cells from pVAX1-*cpc*/CL (MPL) vaccinated mice increased 2-2.5 folds compared to the naked pVAX1-*cpc* and pVAX1-*cpc*/CL after infectious challenge, reconfirming a better CMI response elicited by MPLA-liposomal DNA vaccine regimen compared to all other experimental groups ($p < 0.001$) (Fig. 5B). Taken together, these finding suggest that the MPLA-liposomes can significantly enhance the DTH and T cell proliferation induced by DNA vaccination, over cationic liposomes without MPLA for improved protection.

3.7. Effects of MPLA-bearing cationic liposomes on activation of dendritic cells

Recent advances in vaccinology suggest host DCs and TLRs to be innate targets for initiating a strong vaccine induced adaptive immunity [50]. As shown in Fig. 5C, MPLA-liposomes adjuvant itself i.e. CL (MPL) induced a significant enhancement of CD40 ($p < 0.05$), CD86 ($p < 0.05$) and CD80 ($p < 0.001$) expression profiles on splenic DCs, which were further enhanced after entrapment of pVAX1-*cpc* within these liposomes. Notably, MHC class II expression, regarded as a biomarker of enhanced antigen presentation, was also significantly enhanced by CL (MPL) ($p < 0.05$) and pVAX1-*cpc*/CL (MPL) ($p < 0.0001$) vaccinated

groups. Further, including MPLA within lipid backbone of cationic liposomes i.e. pVAX1-*cpc*/CL (MPL) immunization significantly enhanced the expression of CD40 ($p < 0.001$), CD86 ($p < 0.0001$) and MHCII ($p < 0.001$), over pVAX1-*cpc*/CL immunized animals. Hence, our pilot study indicated that including a TLR4 ligand like MPLA within lipid backbone of DSPC liposomes resulted in enhanced antigen presentation by DCs which may specifically result in elicitation of *Leishmania*-specific T cell responses after infection. Hence this adjuvant formulation can be used for a DNA vaccine to trigger both innate and adaptive response for sustained immunity.

3.8. Enhanced IgG2a over IgG1 before challenge predicts successful vaccination

As in active VL, increased IgG1 usually characterizes the Th2 response and disease progression, while increase in IgG2a is indicative of Th1 response and parasite clearance [51]; we measured both these IgG isotypes as surrogates of *in vivo* protection. Following DNA immunization, rCPC –specific IgG1 and IgG2a were increased in all mice throughout the experimental period. Importantly, highest ratio of IgG2a:IgG1 ($p < 0.05$) was elicited in pVAX1-*cpc*/CL (MPL) immunized group compared to those that received naked pVAX1-*cpc* and liposomal pVAX1-*cpc* without MPLA (supplementary Table. S1). At 3 months post-infection, there was an increase rCPC –specific serum IgG in all the experimental groups; being significantly high ($p < 0.001$) in pVAX1-*cpc*/CL and pVAX1-*cpc*/CL (MPL) immunized animals, compared to controls (data not shown). Notably, two to four-fold higher anti-rCPC IgG2a levels were detected in the sera of pVAX1-*cpc*/CL and pVAX1-*cpc*/CL (MPL) groups compared to infected controls. In contrast, mice immunized with empty liposomes i.e. CL, CL(MPL) and naked pVAX1-*cpc* had similar IgG2a: IgG1 ratio after infection, lower than pVAX1-*cpc*/CL, revealing a lack of Th1 dominance. The combined IgG1 and IgG2a production with highest IgG2a:IgG1 ratio was observed in MPLA-liposomal

DNA immunized group, disclosing a Th1-biased mixed Th1/Th2 immune protection by this liposomal vaccine.

3.9. Vaccination with MPLA-liposomal pVAX1-*cpc* showed enhanced protection against VL

Although immune measurements usually correlate with protective efficacy, the ultimate test for any vaccine is the control of *in vivo* infection. Both pVAX1-*cpc*/CL and pVAX1-*cpc*/CL (MPL)-immunized mice exhibited a positive correlation between reduced parasite burden and hepato- and splenomegaly, 3 months after *L. donovani* challenge (Fig. 6A). The MPLA pVAX1-*cpc*/CL (MPL) immunization, however, demonstrated significant reduction in liver ($p < 0.0001$) and spleen ($p < 0.05$) weight in comparison to liposomal DNA vaccine without MPLA (Fig. 6A). Notably, in pVAX1-*cpc*/CL and pVAX1-*cpc*/CL (MPL)-immunized animals, liver parasite burden were inhibited by 80% and 97% (Fig. 6B) and the splenic parasite burden were reduced by 71.6% and 98 % (Fig. 6B) and, respectively, 90 days after infection compared with naked pVAX1-*cpc* DNA immunized animals. Moreover, pVAX1-*cpc*/CL(MPL) immunization resulted in maximal reduction in LDU, in liver and spleen, which were significantly lower ($p < 0.05$) than liposomal DNA immunization without MPLA (Fig. 5B). As shown in Fig. 6B, empty liposomes with MPLA could suppress *L. donovani* infection only upto 16.4% in the liver, with negligible effect against parasites in the spleen. Immunization with naked pVAX1-*cpc* resulted in about 65% and 68% suppression in the liver and spleen parasite load, respectively ($p < 0.0001$), compared to the infected controls. Representative Giemsa-stained stamped smears of liver and spleen (Fig. 6C and supplementary Fig. S4) also demonstrates the superior efficacy of pVAX1-*cpc*/CL (MPL) immunized mice in intracellular amastigote clearance.

LDA analysis also revealed the presence of very low number of viable parasites in spleen by immunization with pVAX1-*cpc*/CL(MPL) (almost 10^9 fold reduction in parasite load),

followed by pVAX1-*cpc*/CL and pVAX1-*cpc* (almost 10^{6-7} fold reduction in parasite load), compared to infected controls, $p < 0.0001$ (Fig. 6D). Mice receiving different liposomal pVAX1-*cpc* DNA vaccine formulations showed comparable levels (almost 10^{7-8} fold reductions in parasite load compared to infected controls, $p < 0.0001$) of protection in the liver (Fig. 6D). Notably, about 10^5 fold reduction compared to PBS ($p < 0.0001$) in hepatic parasite burden was also detected in mice immunized with MPLA-liposomes alone.

In conjunction (Fig. 6E and F), we found significantly elevated proportion of IL-12^+ $CD4^+$ and $CD8^+$ T cells increased significantly in all pVAX1-*cpc* DNA immunized groups, after challenge, compared to infected controls, as analyzed using Student's t-test. The percentage of IL-12^+ T cells in pVAX1-*cpc*/CL (MPL) immunized group was significantly higher not only in comparison to controls, but also to the naked pVAX1-*cpc* ($p = 0.004$ for $CD3^+CD4^+$IL-12^+ cells and $p = 0.0024$ for $CD3^+CD8^+$IL-12^+ cells) and pVAX1-*cpc*/CL (p= 0.0219 for $CD3^+CD4^+$IL-12^+ cells and p= 0.0466 for $CD3^+CD8^+$IL-12^+ cells) groups. In contrast, the percentage of IL-10^+ $CD4^+$ and $CD8^+$ T cells decreased in all liposomal DNA immunized mice (Fig. 6E and F), with highest suppression in pVAX1-*cpc*/CL (MPL) group compared to infected controls (p= 0.0001 for $CD3^+CD4^+$IL-10^+ cells and p= 0.0004 for $CD3^+CD8^+$IL-10^+ cells) as well as pVAX1-*cpc*/CL group (p= 0.009 for $CD3^+CD4^+$IL-10^+ cells and $p = 0.001$ for $CD3^+CD8^+$IL-10^+ cells) after infection. Percentage of IL-10^+ T cells did not differ significantly from infected controls in naked pVAX1-*cpc* immunized group. Moreover, pVAX1-*cpc*/CL (MPL) immunization also resulted in significant lowering of IL-4^+ $CD4^+$ and $CD8^+$ T cell populations (p= 0.003 for $CD3^+CD4^+$IL-4^+ cells and p= 0.001 for $CD3^+CD8^+$IL-4^+ cells) over infected controls.

3.10. Immunomodulatory activities of pVAX1-*cpc* entrapped in MPLA-liposomes

Since balance between pro- (mainly IFN-γ and IL-12) and anti-inflammatory (mainly IL-10, TGF-β and IL-4) cytokines play a crucial role in clinical outcome of active VL [52], we analyzed their induction in splenocytes of immunized mice before and after *L. donovani* infection. Compared to naked pVAX1-*cpc*, immunization with pVAX1-*cpc* in MPLA-liposomes significantly ($p < 0.0001$) augmented secretion of rCPC-specific Th1-related cytokines including IFN-γ and IL-12 (Fig. 7, A and B), both before and after infection. The level of IFN-γ and IL-12 was suppressed in the infected controls (105 ± 10.41 and 153.3 ± 12.02), but were increased significantly in pVAX1-*cpc* (535.0 ± 58.95 and 346.7 ± 29.06), pVAX1-*cpc*/CL (680 ± 41.63 and 556.7 ± 34.8) and pVAX1-*cpc*/CL (MPL) (1133 ± 44.1 and 760 ± 23.09) after infection. On contrary, the levels of Th1-suppressive cytokines like IL-4, IL-10 and TGF-β remained unaffected in immunized animals compared to controls (Fig. 7, C-E). Their levels, however, were increased in general after challenge in all groups, although pVAX1-*cpc* DNA immunized groups (with or without liposomes), produced lower levels of these Th2 cytokines compared to infected controls. As shown in Figure 7 (C-E), at 3 months post-infection, mice immunized with pVAX1-*cpc*/CL (MPL) showed almost 2.6 fold, 4 fold and 7 fold reductions in IL-10, IL-4 and TGF-β, respectively, compared to infected controls. The results demonstrate that the MPLA-liposomal DNA vaccine induces high-level of Th1 responses against *L. donovani* antigen, which are further augmented after infection correlating with the strong protective immunity seen in the previous experiments. As shown in Fig. 7F and G respectively, the IFN-γ/IL-4 and IFN-γ/IL-10 ratios were in general higher in immunized mice than in naive or infected controls. Further, the IFN-γ/IL-4 and IFN-γ/IL-10 ratios were significantly ($p < 0.0001$) enhanced by MPLA-liposomal pVAX1-*cpc* DNA vaccine above the levels of the naked pVAX1-*cpc* and liposomal pVAX1-*cpc* without MPLA, both before and after challenge (Fig. 7F-G).

3.11. Induction of multifunctional Ag-specific T cells correlates with protective immunity

Antigen-specific T cells producing multiple Th1-related cytokines simultaneously (polyfunctional T cells) appear to be especially effective against *Leishmania*, as reported earlier [53]. Vaccine induced multifunctionality of $CD4^+$ and $CD8^+$ T cells in various combinations was characterized by rCPC –specific intracellular IL-2, TNF-α and IFN-γ using multiparametric FACS)[54] and Boolean gating (supplementary Fig. S3), 3 months post-infection (Fig. 8). Our results clearly showed that pVAX1-*cpc*/CL (MPL) immunized mice induced a significantly higher percentage of triple cytokine (IFN-γ^+TNF-α^+IL-2^+) producing $CD4^+$ (Fig. 8B and C) and $CD8^+$ (Fig. 8E and F) T cells compared to any other group. Further, almost similar percentage of double cytokine positive (IFN-γ^+IL-2^+) $CD4^+$ (Fig. 8B) and $CD8^+$ (Fig. 8E) cells were also found in pVAX1-*cpc*/CL (MPL) immunized animals in comparison to the triple-positive cells. pVAX1-*cpc*/CL (MPL) immunization generated a significantly higher frequency (0.8%) of double cytokine (IFN-γ^+TNF-α^+) positive $CD4^+$ T cells above their PBS controls, whereas the pVAX1-*cpc*/CL vaccine could only increase the IFN-γ and TNF-α-single producers to 1.3 and 0.42 %, respectively. However, both the liposomal DNA vaccines generated significantly higher percentage (0.8%) of the double-positive (IFN-γ^+TNF-α^+) $CD8^+$ T cells (Fig. 8E). A comparatively higher population of single-positive (IFN-γ^+, or IL-2^+) $CD4^+$ and $CD8^+$ T cells were found in both pVAX1-*cpc*/CL and pVAX1-*cpc*/CL (MPL) immunized animals above the triple-positive cells. On the other hand, the mice receiving naked pVAX1-*cpc* showed a modest increase in the proportion of both IFN-γ^+ or IL-2^+ -single cytokine positive $CD4^+$ (Fig. 8B and C) and $CD8^+$ (Fig. 8E and F) T cells, without any significant enhancement in double or triple-positive cells. In contrast to the negligible correlation observed between the total proportions of $CD4^+$ and $CD8^+$ T

cells producing IFN-γ alone or in combination with another cytokine (Fig.8B and E), which ranged below 1.2%, our study revealed a positive correlation between the percentage of triple positive (IFN-γ^+TNF-α^+IL-2^+) $CD4^+$ and $CD8^+$ T cells and degree of protection. The qualitative differences in T cell response are pictorially represented by pie charts (Fig. 8C and F) for different immunized groups. Determination of the total percentage of $CD4^+$ (Fig. 8C) T cells producing all three (IFN-γ^+TNF-α^+IL-2^+) cytokines, any two, or any one cytokine, it is observed that over 90% of the total T cells in infected and adjuvant [i.e. CL and CL(MPL)] controls comprised of single cytokine-positive cells, while about 30% and 10% of the response in pVAX1-*cpc*/CL (MPL) vaccine came from double and triple-positive cells, respectively. Regarding the total cytokine produced from $CD8^+$ T cells (Fig. 8F), it is observed that while negligible triple- positive cells were found in the infected mice, its proportion increased in all immunized mice and peaked in the pVAX1-*cpc*/CL (MPL) group (13%), followed by pVAX1-*cpc*/CL (6%). Also, about 68% and 20% of the response to pVAX1-*cpc*/CL (MPL) vaccination was single positive and double positive cells respectively (Fig. 8F). Therefore, the proportion of the triple- positive T cells increased for protected groups at the expense of the single- and double-positive cells, compared to controls. Collectively, our data reveals that vaccination with MPLA-liposomal pVAX1-*cpc* vaccine elicits highest proportion of triple cytokine positive (IFN-γ^+TNF-α^+IL-2^+) $CD4^+$ and $CD8^+$ T cells, predictive of protection. Further, a Th1-biased response driven by both $CD4^+$ and $CD8^+$ T cells types is required for protection following vaccination.

3.12. MPLA-liposomal pVAX1-*cpc* elicits robust memory generation in immunized mice

Memory T cells have been considered as a reliable biomarker to assess vaccine-induced long-term protection against leishmaniais [54]. Based on the memory differentiation markers CD44 and CD62L., we determined the generation of naive ($CD44^{low}$ $CD62L^{high}$), central memory

(CD44^{high} CD62L^{high}, T_{CM}) and effector memory (CD44^{high} CD62L ^{low}, $T_{EFF/EM}$) subsets in $CD4^+$ and $CD8^+$ T cells from immunized mice, to assess long-lasting immunity. As shown in Fig. 9 (B-E), the subtle co-expression of CD44 and CD62L i.e.CD44^{high} CD62L^{high}, T_{CM} were low in infected controls (1.6% of $CD4^+$ and 4.56% of $CD8^+$ T cells), which was upregulated in pVAX1-*cpc*/CL (3.96% of $CD4^+$ and 10.8% of $CD8^+$ T cells) and pVAX1-*cpc*/CL (MPL) (6.76% of $CD4^+$ and 27.4% of $CD8^+$ T cells) vaccinated groups. Naked DNA immunization with pVAX1-*cpc* had negligible effect on inducing central memory (T_{CM}) cells (2.88% of $CD4^+$ and 8.97% of $CD8^+$ T cells). Moreover, the percentage of effector memory cytotoxic T cells (CD44^{high} CD62L ^{low}, $T_{EFF/EM}$) was significantly increased in pVAX1-*cpc* (73.3% of $CD4^+$ and 53.9% of $CD8^+$ T cells), pVAX1-*cpc*/CL (72.8% of $CD4^+$ and 69.1% of $CD8^+$ T cells) and pVAX1-*cpc*/CL (MPL) (87% of $CD4^+$ and 65.9% of $CD8^+$ T cells) vaccinated groups, compared to infected controls (23.4% of $CD4^+$ and 40.6% of $CD8^+$ T cells). Notably, MPLA-liposomal DNA vaccination elicited overall statistically significant percentage of CD44^{high} CD62L^{high}, T_{CM} cells ($p < 0.001$) (Fig. 9E) in concordance with resolution of disease and durable protection.

To evaluate the functional killing capacity of the effector memory (CD44^{high} CD62L^{low}, $T_{EFF/EM}$) $CD4^+$ and $CD8^+$ T cells, the frequency of IFN-γ^+ T cells, as an important predictor of parasite clearance by [55] was analyzed after infection. Mice immunized with pVAX1-*cpc* in cationic liposomes with MPLA had much higher level of IFN-γ producing T cells than mice receiving pVAX1-*cpc* alone or entrapped in cationic liposomes without MPLA or (Fig. 9F). Notably, this IFN-γ functionality of $CD8^+$ T cells is significantly higher compared to $CD4^+$ T cells ($p < 0.05$) in pVAX1-*cpc*/CL (MPL) immunized group.

4. Discussion

Successful clinical application of anti-leishmanial immunoprophylaxis necessitates enhanced T cell-mediated parasite clearance and memory. Although several leishmanial vaccine candidates including ORFF, A2, KMP-11, cysteine proteases, H2A, H2BH3, H4, LACK, nucleoside hydrolase 36, proteophosphoglycan, have been tested against VL with varying success rates, they were poorly immunogenic towards the elicitation of $CD8^+$ T cell responses compared to those for live vaccines studied in higher preclinical models [3, 56].

In general, the key issues involved in intracellular DNA delivery are problems in the cellular internalization of large charged molecules like DNA and also their bioavailability at the target sites, avoiding the biological barriers. Cationic liposomes have emerged as an ideal delivery system carrying DNA and interacting with the negatively charged cell surface for successful endocytosis-mediated uptake [57] while protecting the entrapped DNA against nucleases by its lipid bilayers [58]. Since liposomal efficacy largely depends on suitable immunostimulatory adjuvants to generate the appropriate adaptive immunity in human permissible routes of administration [17, 59], we incorporated the adjuvant MPLA in the lipid-bilayer of delivery vesicles. MPLA, a detoxified lipopolysaccharide (endotoxin) from *Salmonella minnesota*, is a TLR4 agonist, used in several human clinical trials [19]. As the vaccine candidate we chose leishmanial Cysteine protease type III (*cpc*) that has shown appreciable protection in preclinical evaluations against *L. infantum* [20] and *L. donovani* [18].

Our studies show that the novel cationic liposomal system provided many advantages for gene delivery. AFM, DLS analysis and cryo-TEM showed that the MPLA-liposomes encapsulating pDNA had a mean diameter of < 200 nm, which may be advantageous than the large-sized vesicles against *Leishmania* [42, 60] for easy lymph node entry, reduced particle aggregation and good intracellular uptake mostly through macropinocytosis and clathrin-mediated pathways [18]. Moreover, such small-sized vesicles can be terminally filtered thus avoiding any aseptic manufacturing. Most probably the electrostatic interaction between

cationic lipids and the anionic pDNA inside the MPLA-liposomes correlates with its high transfection efficacy, stability and impressive immune responses against *Leishmania*. MΦs are important phagocytes playing dual role in terms of host susceptibility and resistance to *Leishmania* infection [61]. MPLA-liposomal DNA vaccine most effectively arrested the *in vitro L. donovani* multiplication by activating the peritoneal MΦs so as to initiate and maintain the protective immunity. Further, the MPLA-liposomes were able to transfect RAW 264.7 MΦ cell line efficiently without any significant cytotoxicity. As shown in CLSM studies there was increased uptake of Rh123 MPLA-liposomes encapsulating labelled pDNA into the infected MΦs compared with the uninfected ones, which is may be due to altered metabolism and phagocytic behaviour of *Leishmania*-infected MΦs towards ingestion of particulate material. Accumulation of some internalized liposomes were observed even after 6h after addition (data not shown), pDNA persistence inside the host cells, for efficient DNA delivery and antileishmanial therapy. Since successful prophylaxis depends on both the efficient immunization as well as innate immune status of the host, the most promising approach for VL elimination would be to stimulate the innate immunity in addition to adaptive response. Along with MΦs, DCs are crucial antigen presenting cells for initiating T cell immunity against *Leishmania,* chiefly via DC-derived IL-12. Elevated CD80/86 and CD40 expressions are required for necessary T cell activation whereas increased surface expression of MHCII signifies optimum antigen presentation to the $CD4^+$ T cells. Functional impairment of activation and maturation of DCs has long been associated with parasite replication during murine VL [62]. As observed, naked DNA vaccine lead to moderate DC activation above the PBS controls. However, incorporating MPLA into conventional DSPC-liposomes resulted in significant enhancement of DC maturation. In fact, it appears that the naked pDNA (also CpG-enriched relative to mammalian DNA) has some intrinsic adjuvant properties triggering mainly the TLR9 receptors on DCs, as reported earlier [63], which is

synergistically enhanced by the MPLA-liposomes that signal through TLR4 to activate APCs. Hence, our results are supportive of the fact that the preceding innate immunity, operating through several TLRs, modulates the strength and quality of adaptive response following chronic infections [64-66], which are often synergistic [66]. Consistent with a recent study with DOTAP and hyaluronic acid nanoparticles [67], the innate stimulation of DCs by our MPLA-liposomes through co-stimulatory signals like CD80, CD86 and CD40 eventually help in IFN-γ, IL-6 and IL-12 secretion, subsequent lymphocyte activation and proliferation for optimum adaptive response. Based on these preliminary results, we next investigated the adjuvant potency of these MPLA-liposomes for DNA vaccination with Ld*cpc* as a model antigen. Since anti-leishmanial immunity depends largely on parasite persistence, vaccine success definitely warrants robust immune response elicited against the disease onset rather than sterile protection [5, 68]. We report that MPLA-liposomal pVAX1-*cpc* strengthens host immunity at various levels. In this study, Ld*cpc*-based DNA immunization with MPLA-liposomes shows 97%-98% reduction in parasite burden in liver and spleen of BALB/c infected with *L. donovani*. Current vaccine formulation achieved better protection than reported by us earlier [18] where, immunization with liposomal rCPC alone reduced the splenic parasite burden in by 91% in comparison to the infected controls. Such a high level of protection has not been achieved by any other single antigen DNA vaccine against experimental VL, except for a recent report by Guha et al. [69].

It is well-established that in mice IFN-γ and IL-4 directly regulates the class-switching in B cells to IgG2a and IgG1 respectively[70].We found that immunization of MPLA-liposomal DNA vaccine generated 4-fold higher levels of anti-CPC IgG2a with decreased IgG1 levels in immunized animals compared to controls, after infection. In addition, the anti-parasite IgG isotypes induced in response to the liposomal DNA vaccine, IgG2a in excess of IgG1, as well as the high IFN-γ/IL-10 or IL-4 ratio seen in immunized animals indicate a strong Th1 biased

immunity typically resembling the human situation that correlates with disease resolution. Although a clear Th1/Th2 dichotomy is absent in the rodent models of VL, protective immunity is driven by IFN-γ and IL-12. In human VL, active disease is associated with skewing of immune response towards IL-4, IL-10 and TGF-β secreting Th2 and/or regulatory T cells, whereas protective immunity depends on enhanced secretion of Th1 cytokines like IL-12, IFNγ and TNF-αtogether with downregulation of IL-10 and TGF-β.

5. Conclusion

Our results demonstrated a dominant Th1 response elicited by pVAX1-*cpc*/CL(MPL) as denoted by the enhanced IL-12 and IFN-γ. Multifunctional T cells play a vital role in raising protective immunity against a variety of intracellular pathogenic organisms including *Leishmania*, where vaccine-induced protection is usually depends on activation of $CD4^+$ and $CD8^+$ T cells producing IFN-γ [53]. Conversely, chronic VL is characterized by a prominent T cell dysfunction which parallels the progressive increase in parasite burden [58, 83]. We observed that $CD4^+$ and $CD8^+$ T cells induced by MPLA-liposomal pVAX1-*cpc* immunization exhibited a clear Th1 profile *ex vivo* and contained significantly higher polyfunctional populations simultaneously producing IFN-γ, TNF-α, and IL-2 after infection, compared to all other immunized groups. In addition, the large proportion of multifunctional $CD8^+$ T cells generated in these mice probably contributes to clearance of intracellular parasites thereby inducing a durable immunity against VL. The protective immunity following liposomal pVAX1-*cpc* vaccine regimen clearly correlated with enhanced IFN-γ and IL-12 produced from $CD3^+$ T cells. However, despite the increased IFN-γ and IL-12 production, lack of IL-10 suppression in naked pVAX1-*cpc* immunized mice apparently overrode any protective immunity exerted by these Th1 cytokines correlating with lower efficacy of the DNA vaccine without adjuvant.

Although the protective role of $CD8^+$ T cells in experimental cutaneous leishmaniasis is still controversial, their role in maintaining long-term memory has been reported against VL [10]. MPLA-liposomal pVAX1-*cpc* generated the highest proportion of central memory ($CD44^{high}CD62L^{high}$, T_{CM}) $CD4^+$ and $CD8^+$ T cells, compared to all other study groups. Our findings are in consistence with the previous studies [68] showing important contributions of the central memory cells in maintaining protective immunity even without parasite persistence. Overall the strong immunomodulatory properties and CMI response shown by these MPLA-liposomes coupled with desired antigen (s) may open a new avenue for addressing both $CD4^+$ and $CD8^+$ T cell-based immune response against many other diseases and cancer.

Acknowledgements

This work was supported by the Council of Scientific and Industrial Research (CSIR) grant (No.BSC0114). A.D is a CSIR Fellow. We are thankful to Siddhartha Roy and Samit Chattopadhay, the past and present director, CSIR-IICB, India for supporting this work. Authors are grateful to Jayati Sengupta for the cryo-EM work. We thank Muruganand for AFM experiments and Diptadeep Sarkar for excellent technical assistance in the confocal microscopy studies. We warmly acknowledge Janmenjoy Midya for assisting in the animal experiments.

Conflicts of Interest

The authors declare no conflict of interest.

Author Contributions

A.D. and N.A. secured funding, conceptualized and designed the study. A.D., M.A., A.S and N.D. conducted the experiments. A.D. and M.A. contributed reagents/materials. A.D. and

N.A. analyzed the data, interpreted the results and wrote the manuscript. All the authors reviewed and approved the manuscript.

References

(1) Ready, P.D. Epidemiology Of Visceral Leishmaniasis. *Clin. Epidemiol*. **2014**, *6,* 147–154.

(2) Mathers, C.D.; Ezzati, M.; Lopez, A.D. Measuring The Burden Of Neglected Tropical Diseases: The Global Burden Of Disease Framework. *PLoS. Negl. Trop. Dis*. **2007**, *1,* e114.

(3) Croft, S. L.; Olliaro, P. Leishmaniasis Chemotherapy— Challenges and Opportunities. *Clin. Microbiol. Infect.* **2011**, *17*, 1478–1483.

(4) Gurunathan, S.; Klinman, D.M.; Seder, R.A. DNA Vaccines: Immunology, Application, and Optimization. *Annu. Rev. Immunol*. **2000**, *18*, 927–974.

(5) Handman, E. Leishmaniasis: Current Status of Vaccine Development. *Clin. Microbiol. Rev*. **2001**, *14*, 229–243.

(6) Riede, O.; Seifert, K.; Oswald, D.; Endmann, A.; Hock, C.; Winkler, A., Salguero, F.J., Schroff , M., Croft, S.L., Juhls, C. Preclinical Safety and Tolerability of a Repeatedly Administered Human Leishmaniasis DNA Vaccine. *Gene. Ther.* **2015**, *22*, 628–635.

(7) Seifert, K.; Juhls, C.; Salguero, F.J.; Croft, S.L. Sequential Chemoimmunotherapy of Experimental Visceral Leishmaniasis Using a Single Low Dose of Liposomal Amphotericin B and a Novel DNA Vaccine Candidate. *Antimicrob. Agents. Chemother*. **2015**, *59,* 5819–5823.

(8) Kumar, A.; Samant, M. DNA Vaccine against Visceral Leishmaniasis: A Promising Approach for Prevention and Control. *Parasite. Immunol*. **2016**, *38,* 273–281.

(9) Ferraro, B.; Morrow, M. P.; Hutnick, N. A.; Shin, T. H.; Lucke, C. E.; Weiner, D. B. Clinical Applications of DNA Vaccines: Current Progress. **2011**, *Clin. Infect. Dis*. *53,* 296–302.

(10) Stäger, S.; Rafati, S. $CD8^+$ T Cells in *Leishmania* Infections: Friends or Foes? *Front. Immunol.* **2012**, *3*:5.

(11) Mazumder, S.; Maji, M.; Ali, N. Potentiating Effects of MPL on DSPC Bearing Cationic Liposomes Promote Recombinant GP63 Vaccine Efficacy: High Immunogenicity and Protection. *PLoS. Negl. Trop. Dis*. **2011**, 5, e1429.

(12) Maji, M.; Mazumder, S.; Bhattacharya, S.; Choudhury, S.T.; Sabur, A.; Shadab, M., Bhattacharya, P., Ali, N. A Lipid Based Antigen Delivery System Efficiently Facilitates MHC Class-I Antigen Presentation in Dendritic Cells to Stimulate CD8(+) T Cells. *Sci. Rep*. **2016**, *6,* 27206.

(13) Korsholm, K.S.; Andersen, P.; Agger, E.M. Cationic Liposomes as Vaccine Adjuvants. *Expert. Rev. Vaccines*. **2011**, *10,* 513–521.

(14) Radler, J.O.; Koltover, I.; Salditt, T.; Safinya, C.R. Structure of DNA–Cationic Liposome Complexes: DNA Intercalation in Multilamellar Membranes in Distinct Interhelical Packing Regimes. *Science*. **1997**, *275,* 810 –814.

(15) Zuhorn, I.S.; Hoekstra, D. On the Mechanism of Cationic Amphiphile Mediated Transfection. To Fuse or Not To Fuse: Is that the Question? *J. Membr. Biol*. **2002**, *189,* 167–179.

(16) Yasuda, K.; Ogawa, Y.; Yamane, I.; Nishikawa, M.; Takakura,Y. Macrophage Activation by a DNA/Cationic Liposome Complex Requires Endosomal Acidification and TLR9- Dependent and -Independent Pathways. *J. Leukocyte. Biol*. **2005**, *77*, 71–70.

(17) Bhowmick, S.; Mazumdar, T.; Ali, N. Vaccination Route that Induces Transforming Growth Factor Beta Production Fails to Elicit Protective Immunity against *Leishmania donovani* Infection. *Infect. Immun*. **2009**, *77,* 1514–1523.

(18) Das, A.; Ali, N. Combining Cationic Liposomal Delivery With MPL-TDM For Cysteine Protease Cocktail Vaccination Against *Leishmania Donovani*: Evidence For Antigen Synergy And Protection. *PLoS. Negl. Trop. Dis*. **2014**, *8,* 1–17.

(19) Reed, S. G; Hsu, F.; Carter, D.; Orr, M.T. The Science of Vaccine Adjuvants: Advances in TLR4 Ligand Adjuvants. *Curr. Opin. Immunol*. **2016**, *41,* 85–90.

(20) Khoshgoo, N.; Zahedifard, F.; Azizi, H.; Taslimi, Y.; Alonso, M.J.; Rafati, S. Cysteine Proteinase Type III Is Protective Against *Leishmania infantum* Infection In BALB/C Mice And Highly Antigenic In Visceral Leishmaniasis Individuals. *Vaccine*. **2008**, *26,* 5822–5829.

(21) Doroud, D.; Zahedifard, F.,; Vatanara, A.; Najafabadi, A.R.; Taslimi, Y.; Vahabpour, R., Torkashvand, F., Vaziri, B., Rafati, S. Delivery of a Cocktail DNA Vaccine Encoding Cysteine Proteinases Type I, II and III with Solid Lipid Nanoparticles Potentiate Protective Immunity against *Leishmania major* Infection. *J. Control. Release*. **2011**, *153,* 154–162.

(22) Rafati, S.; Fasel, N.; Masina, S. *Leishmania* Cysteine Proteinases: from Gene to Subunit Vaccine. *Curr. Genom*. **2003**, *4,* 253–261.

(23) Bart, G.; Frame, M.J.; Carter, R.; Coombs, G.H.; Mottram, J.C. Cathepsin B-Like Cysteine Proteinase-Deficient Mutants of *Leishmania mexicana*. *Mol. Biochem. Parasitol*. **1997**, *88,* 53–61.

(24) Somanna, A.; Mundodi, V.; Gedamu, L. Functional Analysis Of Cathepsin B Like Cysteine Proteases From *Leishmania Donovani* Complex. Biol. Chem. **2002**, *28,* 25305–25312.

(25) Afrin, F.; Ali, N. Adjuvanticity and Protective Immunity Elicited by *Leishmania donovani* Antigens Encapsulated in Positively Charged Liposomes. *Infect. Immun*. **1997**, *65,* 2371–2377.

(26) Bhowmick, S.; Ravindran, R.; Ali, N. Gp63 In Stable Cationic Liposomes Confers Sustained Vaccine Immunity To Susceptible BALB/C Mice Infected With *Leishmania donovani*. *Infect. Immun*. **2008**, *76,* 1003–1015.

(27) Harmon P, Cabral-Lilly D, Reed RA, Maurio FP, Franklin JC, Janoff A. The Release and Detection of Endotoxin from Liposomes. *Anal. Biochem*. **1997**, *250*, 139–146.

(28) Wagenknecht, T.; Grassucci, R.; Frank, J. Electron Microscopy and Computer Image Averaging Of Ice-Embedded Large Ribosomal Subunits from *Escherichia coli*. *J. Mol. Biol.* **1988**, *199,* 137–147.

(29) Wheeler, J.J.; Palmer, L.; Ossanlou, M.; MacLachlan, I.; Graham, R.W.; Zhang, Y.P. Hope, M.J., Scherrer, P., Cullis, P.R. Stabilized Plasmid-Lipid Particles: Construction and Characterization. *Gene. Ther.* **1999**, *6,* 271–281.

(30) Heyes, J.; Hall, K.; Tailor V.; Lenz, R.; MacLachlan, I. Synthesis and Characterization of Novel Poly(Ethylene Glycol)-Lipid Conjugates Suitable for Use in Drug Delivery. *J. Control. Release.* **2006**, *112,* 280–290.

(31) Mazumdar, T.; Anam, K.; Ali, N. A Mixed Th1/Th2 Response Elicited by a Liposomal Formulation of *Leishmania* Vaccine Instructs Th1 Responses and Resistance to *Leishmania donovani* in Susceptible BALB/c mice. *Vaccine*. **2004**, *22,* 1162–1171.

(32) Kar, S.; Sharma, G.; Das, P.K. Fucoidan Cures Infection with Both Antimony-Susceptible and -Resistant Strains Of *Leishmania donovani* Through Th1 Response and Macrophage-Derived Oxidants. *J. Antimicrob. Chemother*. **2011**, *66,* 618– 625.

(33) Lyons, A.B. Analysing Cell Division In Vivo and In Vitro Using Flow Cytometric Measurement of CFSE Dye Dilution. *J. Immunol. Methods*. **2000**, *243*, 147–154.

(34) Stauber, L.A.; Franchino, E.M.; Grun, J. An Eight Day Method for Screening Compounds against *Leishmania donovani* in the Golden Hamster. *J. Protozool*. **1958**, *5,* 269–273.

(35) Titus, R.G.; Marchand, M. Boon; T. Louis, J.A. A Limiting Dilution Assay for Quantifying *Leishmania major* in Tissues of Infected Mice. *Parasite. Immunol.* **1985**, *7*, 545–555.

(36) Schwendener, R.A. Liposomes as Vaccine Delivery Systems: A Review of the Recent Advances. *Ther. Adv.Vaccines*. **2014**, *2*, 159–182.

(37) Perrie, Y.; Gregoriadis, G. Liposome-Entrapped Plasmid DNA: Characterization Studies. *Biochim. Biophys. Acta*. **2000**, *1475,* 125–132.

(38) Anderson, R.C.; Fox, C.B.; Dutill, T.S.; Shaverdian, N.; Evers, T.L.; Poshusta, Chesko, J., Coler, R.N., Friede, M., Reed, S.G., Vedvick, T.S. Physicochemical Characterization and Biological Activity of Synthetic TLR4 Agonist Formulations. *Coll. Surf. B: Biointerfaces*. **2010**, *75*, 123–132.

(39) Orr, M.T.; Fox, C.B.; Baldwin, S.L.; Sivananthan, S.J.; Lucas, E.; Lin, S. Phan T1, Moon, J.J., Vedvick, T.S, Reed, S.G., Coler, R.N. Adjuvant Formulation Structure and Composition are Critical for the Development of an Effective Vaccine against Tuberculosis. *J. Control. Release*. **2013**, *172,* 190–200.

(40) Li, X.; Sloat, B.R.; Yanasarn, N.; Cui, Z. Relationship between the Size of Nanoparticles and their Adjuvant Activity: Data from a Study with an Improved Experimental Design. *Eur. J. Pharm. Biopharm*. **2011**, *78,*107–116.

(41) Joshi, V.B.; Geary, S.M.; Salem, A.K. Biodegradable Particles as Vaccine Antigen Delivery Systems for Stimulating Cellular Immune Responses. *Hum.Vaccines Immunother*. **2013**, *9,* 2584–2590.

(42) Bachmann, M.F.; Jennings, G.T. Vaccine Delivery: A Matter of Size, Geometry, Kinetics and Molecular Patterns. *Nat. Rev. Immunol*. **2010**, *10,* 787–796.

(43) Borborema, S.E.; Schwendener, R.A.; Osso Jr, J.A.; de Andrade Jr, H.F., do Nascimento, N. Uptake And Antileishmanial Activity Of Meglumine Antimoniate-

Containing Liposomes in *Leishmania* (*Leishmania*) *major*-Infected Macrophages. *Int. J. Antimicrob. Agents*. **2011**, *38,* 341–347.

(44) Sinha, R.; Roychoudhury, J.; Palit, P.; Ali, N. Cationic Liposomal-Sodium Stibogluconate (SSG): A Potent Therapeutic Tool For The Treatment Of SSG-Sensitive And Resistant *Leishmania donovani* infection. *Antimicrob. Agents. Chemother*. **2015**, *59,* 344–355.

(45) Legendre, J.Y.; Szoka Jr, Fe. Liposomes for Gene Therapy. In *Liposomes, New Systems and New Trends in their Applications*; Editions de Sante, F. Puissieux, P. Couvreur, J. Delattre, J.P. Devissaugnet, eds. (Paris), **1995**, pp 669–692.

(46) Murray, H.W. Cell-Mediated Immune Response in Experimental Visceral Leishmaniasis. II. Oxygen-Dependent Killing of Intracellular *Leishmania donovani* Amastigotes. *J. Immunol*. **1982**, *129,* 351–357.

(47) Murray, H. W.; Nathan, C. F. Macrophage Microbicidal Mechanisms In Vivo: Reactive Nitrogen Versus Oxygen Intermediates in the Killing of Intracellular Visceral *Leishmania donovani*. *J. Exp. Med*. **1999**, *189,* 741– 746.

(48) Rodrigues, V.; Cordeiro-da-Silva, A.; Laforge, M.; Silvestre, R.; Estaquier, J. Regulation of Immunity During Visceral *Leishmania* Infection. *Parasit Vectors*. **2016**, *9*, 118.

(49) Gautam, S.; Kumar, R.; Singh, N.; Singh, A.K.; Rai, M. Sacks, D., Sundar, S., Nylén, S. CD8 T Cell Exhaustion in Human Visceral Leishmaniasis. *J. Infect. Dis*. **2014**, *209,* 290–299.

(50) Brandonisio, O.; Spinelli, R.; Pepe, M. Dendritic Cells in *Leishmania* Infection. *Microbes. Infect*. **2004**, *6,* 1402–1409.

(51) Deplazes, P.; Smith, N.C.; Arnold, P. H.; Lutz, E.J. Specific IgG1 and IgG2 Antibody Responses of Dogs to *Leishmania infantum* and other Parasites. *Parasite. Immunol*. **1995**, *17,* 451–458.

(52) Ewunetu, T.; Deress,a T.; Gedle, D.; Kumera, G.; Diro, E. Pro- And Anti-Inflammatory Cytokines In Visceral Leishmaniasis. *J. Cell. Sci. Ther*. **2015**, *6:* 206.

(53) Darrah, P.A.; Patel, D.T.; DeLuca, P.M.; Lindsay, R.W.; Davey, D.F.; Flynn, B.J., Hoff, S.T., Andersen, P., Reed, S.G., Morris, S.L., Roederer, M., Seder, R.A. Multifunctional TH1Cells Define a Correlate of Vaccine-Mediated Protection against *Leishmania major*. *Nat. Med*. **2007**, *13,* 843–850.

(54) Zaph, C.; Uzonna, J.; Beverley, S.M.; Scott, P. Central Memory T Cells Mediate Long-Term Immunity To *Leishmania major* In The Absence Of Persistent Parasites. *Nat. Med*. **2004**, *10,* 1104–1110.

(55) Kima, P.E.; Soong, L. Interferon Gamma in Leishmaniasis. *Front. Immunol*. **2013**, *4,* 156.

(56) Kumar, A.; Samant, M. DNA Vaccine against Visceral Leishmaniasis: a Promising Approach for Prevention and Control. *Parasite. Immunol*. **2016**, *38,* 273–281.

(57) Almofti, M.R.; Harashima, H.; Shinohara, Y.; Almofti, A.; Baba, Y.; Kiwada, H. Cationic Liposome-Mediated Gene Delivery: Biophysical Study And Mechanism Of Internalization. *Arch. Biochem. Biophys*. **2003**, *410*, 246–253.

(58) Ibanez, M.; Gariglio, P.; Chavez, P.; Santiago, R.; Wong, C.; Baeza, I. Spermidine-Condensed DNA and Cone-Shaped Lipids Improve Delivery and Expression of Exogenous DNA Transfer by Liposomes. *Biochem. Cell. Biol*. **1996**, *74,* 633–643.

(59) Bhowmick, S.; Ravindran, R.; Ali, N. IL-4 Contributes to Failure, and Colludes with IL-10 to Exacerbate *Leishmania donovani* Infection Following Administration of a Subcutaneous Leishmanial Antigen Vaccine. *BMC. Microbiol*. **2014**, *14:*8.

(60) Carter, K.C.; Dolan, T.F.; Alexander, J., Baillie; A.J., McColgan, C. Visceral

Leishmaniasis: Drug Carrier Characteristics and the Ability to Clear Parasites from the Liver, Spleen and Bone Marrow in *Leishmania donovani* Infected BALB/C Mice. *J. Pharm. Pharmacol*. **1989**, *41,* 87–91.

(61) Buates, S.; Matlashewski, G. General Suppression of Macrophage Gene Expression During *Leishmania donovani* Infection. *J. Immunol.* **2001**, *166,* 3416–3422.

(62) Basu, A.; Chakrabarti, G.; Saha, A.; Bandyopadhyay, S. Modulation Of $CD11C^{+}$ Splenic Dendritic Cell Functions in Murine Visceral Leishmaniasis: Correlation with Parasite Replication in the Spleen. *Immunology.* **2000**, *99,* 305–313.

(63) Dow, S.; Fradkin, L.; Liggitt, D.; Wilson, A.; Heath, T.; Potter, T. Lipid-DNA Complexes Induce Potent Activation Of Innate Immune Responses And Antitumor Activity When Administered Intravenously. *J. Immunol*. **1999**, *163,* 1552–1561.

(64) Kaisho, T.; Akira, S. Toll- like receptor function and signalling. *J. Allergy. Clin. Immunol*. **2006**, *117,* 979–987.

(65) Raman, V.S., Bhatia, A., Picone, A., Whittle, J., Bailor, H.R., O'Donnell, J., Pattabhi, S., Guderian, J.A., Mohamath, R., Duthie, M.S., Reed, S.G. Applying TLR Synergy In Immunotherapy: Implications In Cutaneous Leishmaniasis. *J. Immunol*. **2010**, *185,* 1701–1710.

(66) Shima, F.; Uto, T.; Akagi, T.; Akashi, M. Synergistic Stimulation Of Antigen Presenting Cells Via TLR By Combining Cpg ODN And Poly(Gamma-Glutamic Acid)-Based Nanoparticles As Vaccine Adjuvants. *Bioconjug. Chem*. **2013**, *24,* 926–933.

(67) Fan, Y., Sahdev, P.; Ochyl, L. J.; Akerberg, J.; Moon, J. J. Cationic Liposome-Hyaluronic Acid Hybrid Nanoparticles For Intranasal Vaccination With Subunit Antigens. *J. Control. Release.* **2015***, 208,* 121–129.

(68) Sacks, D. L. Vaccines against Tropical Parasitic Diseases: A Persisting Answer To A Persisting Problem. *Nat Immunol.* **2014**, *15*, 403–405.

(69) Guha, R.; Gupta, D.; Rastogi, R.; Vikram, R.; Krishnamurthy, G.; Bimal, S.; Roy, S.; Mukhopadhyay, A. Vaccination With *Leishmania* Hemoglobin Receptor–Encoding DNA Protects Against Visceral Leishmaniasis. *Sci. Transl. Med.* **2013**, *5,* 1-11.

(70) Coffman, R.L.; Lebman, D.A.; Rothman, P. Mechanism And Regulation Of Immunoglobulin Isotype Switching. *Adv. Immunol*. **1993**, *54,* 229–270.

Figure captions

Figure 1.

Cloning and expression of *L. donovani cpc* in mammalian expression vector pVAX1. (A) Schematic representation of pVAX1-*cpc*. (B) Clone confirmation of *cpc* in pVAX1 vector. Lane 1, λ DNA digested with Hind III marker; lanes 2 & 3, BamHI/HindIII digested pVAX1-*cpc* construct; lane 4, PCR of cloned construct pVAX1-*cpc*; lane 5, PCR of cloned pVAX1-*cpc* construct; lane 5, GeneRuler ™ 1kb DNA ladder marker. (C) RT-PCR analysis for *cpc* in pVAX1-*cpc* transfected HEK293T cells. Lane 1, GeneRuler ™ 1kb DNA ladder marker; lane 2, HEK293T cells without transfection; lane 3, HEK293T cells transfected with vector pVAX1; lanes 4 & 5, HEK293T cells transfected with pVAX1-*cpc*. (D) Expression analysis of Ld*cpc* in transfected HEK293T cell line. Lane 1, western blot of pVAX1-*cpc* transfected HEK293T cells; lane 2, western blot of vector pVAX1 transfected HEK293T cells (E) Coomassie Blue staining of 10% SDS-PAGE. Lane 1, molecular mass marker; lane 2, overexpressed recombinant CPC in *E. coli* BL21(DE3); lane 3, purified recombinant CPC protein.

Figure 2.

Shape and morphology of MPLA cationic liposomes. (A-D) The representative tapping mode images of liposomes captured after 15 min upon deposition on mica. (A) & (B) AFM images represented as amplitude flattened, two-dimensional graphics showing the clean, spherical empty and DNA-loaded MPLA-liposomes, respectively; (C) & (D) Horizontal cross-sections of empty and DNA-loaded MPLA-liposomes indicative of the heights of the vesicles from the base i.e. mica sheet; (E) & (F) three-dimensional images showing empty and DNA-loaded liposomes respectively by AFM study; (G) Cryo-EM micrograph of DSPC-MPLA liposomes, formed at a molar ratio of 7:2:2:0.0016 DSPC:cholesterol:SA:MPLA. The liposome sample was extensively centrifuged to form a pellet, resuspended in 0.02M PBS, and imaged which

shows well-defined, round lipid vesicles having a diameter of 100-250 nm. Original magnification for Cryo-EM was 50×. Scale bar, 100 nm; (H) Schematic representation of DSPC-MPLA liposomes after 3D reconstruction using Amira 3D software. Inset shows a single liposome.

Figure 3.

Cell uptake studies and liposomal antigen presentation. (A) Cellular uptake and intracellular accumulation of MPLA-liposomes encapsulating plasmid pVAX1-*cpc*, by uninfected (left) and infected (right) macrophages (MΦs). Murine peritoneal MΦs were infected *in vitro* with *L. donovani* promastigotes for 3h and subsequently washed and treated with Rh123-MPLA liposomes (green) encapsulating Cy5 (red) labeled pVAX1-*cpc* DNA. Cell nuclei were stained with DAPI (blue). Arrows indicate *L. donovani* amastigotes (small blue dots) inside the infected MΦs. Scale bars, 10 μm. Yellow spots in the merged images indicate the colocalization of liposomes (green) and encapsulated plasmid (red) within the MΦs. The results are representative of two separate experiments; (B) Flowcytometric analysis showing cellular uptake of Rh123-MPLA liposomes in peritoneal MΦs, expressed as histograms representing the fluorescence intensity distribution of MΦs, after 1h, 2h, 3h and 4h of incubation; (C) numerical data representing the mean fluorescence intensity (MFI) ± S.E. of Rh123 fluorescence in MΦs. Data represent one of the three different experiments performed in duplicate. (D) Western blots for TAP1, calregulin, tapasin, cathepsin H, cathepsin S and GILT on extracts of stimulated bone-marrow derived DCs (BMDCs). β-actin served as loading control. BMDCs were stimulated for 18h with empty cationic liposomes with and without MPLA, in RPMI 1640. Unstimulated BMDCs (OM) are taken as controls.

Figure 4.

Stability, toxicity analyses, immunization and anti-leishmanial activity of cationic MPLA liposomes carrying pVAX1-*cpc* DNA. (A) DNase I resistance of the vaccine formulation. Lane 1, plasmid pVAX1-*cpc*; lane 2, pVAX1-*cpc* incubated with active DNAse I for 15min; lane3, pVAX1-*cpc* incubated with active DNAseI for 60 min; lane 4, liposomal pVAX1-*cpc* incubated with active DNAseI for 60 min, followed by lipid extraction; lane5, liposomal pVAX1-*cpc* incubated with active DNAseI for 60 min, without lipid extraction. (B) *In vitro* cell viability assay. Cationic MPLA liposomes (3.2-200 μg/ml w.r.t DSPC) were incubated with murine peritoneal MΦs for 1h, 4h and 12h prior to MTT assay. Values represent mean ± S.E. of four replicates from one of the two similar experiments performed. (C-E) Assessment of *in vivo* toxicity after intravenous administration of DNA vaccine (pVAX1-*cpc*) entrapped in MPLA-liposomes. Serum samples were collected from the BALB/c mice (n=7) after intravenous injection of MPLA-liposomal pVAX1-*cpc* (50 μg and 100 μg w.r.t entrapped plasmid DNA, in single, double or triple doses) dissolved in 0.02 M PBS. Liver function was assayed for the enzymes aspartate transferase (AST) (C), alanine transferase (ALT) (D) and alkaline phosphatase (ALP) (E), as indicators of hepatotoxicity, compared to untreated controls. Data represent mean ± S.E., from one of the two independent experiments. (F) Schematic representation of the immunization protocol. Six-eight weeks old female BALB/c mice were immunized i.m. in the hind leg either with naked plasmid pVAX1-*cpc* (50μg/animal/dose), pVAX1-*cpc* entrapped in cationic liposomes without MPLA or pVAX1-*cpc* entrapped in cationic liposomes with MPLA as adjuvant. Mice were boosted once after 2 weeks. (G) Determination of MΦ activation to suppress *L. donovani in vitro*. Total number of intracellular amastigotes/1000 peritoneal MΦs derived from differently immunized mice were calculated after 72h of in vitro infection with virulent *L. donovani* promastigotes. NO (H) and ROS (I) production by activated MΦs from immunized animals in response to *in*

vitro infection. Data represent mean ± S.E. (n=3), representative of one of the three independent experiments. *$p < 0.05$; ***$p < 0.0001$ in comparison to PBS control, as assessed by one-way ANOVA and Tukey's multiple comparison test. (J) DTH response 1 week after final immunization, expressed as the difference (in mm) between the thickness of the test (rCPC-injected) and control (0.02 M PBS-injected) footpads of same animal after 24h. Data indicate mean ± S.E. (n=5), representative of one of the two independent experiments. ***$p < 0.0001$ compared to PBS controls, as assessed by one-way ANOVA and Tukey's multiple comparison test.

Figure 5.

In vivo immune stimulation by pVAX1-*cpc* entrapped in positively charged DSPC liposomes with or without intrabilayer MPLA. (A) Gating strategy for murine lymphocytes containing CFSE ^{high} and CFSE ^{low} populations, to assess the $CD4^+$ and $CD8^+$ T cell proliferation by flowcytometry. Splenocytes from immunized animals 1 week after booster dose were labeled with CFSE (2μM) and restimulated for 5 days with 2.5μg/ml of rCPC or 2.5μg/ml ConA *in vitro*. Antigen-specific lymphoproliferation from individual animal was analyzed based on CFSE dilution on gated lymphocytes. Boxes on each dot plot indicate the percentage of divided cells (CFSE ^{low}) in each sample. (B) Representative plots from different experimental groups showing percent proliferation of the lymphocytes, calculated in the indicated region (box). (C) The bar graphs show mean percent proliferation of the lymphocytes, which is directly proportional to cell divisions. *$p < 0.05$; **$p < 0.01$; ***$p < 0.001$ compared to PBS controls, as assessed by one-way ANOVA and Tukey's multiple comparison test. Data indicate mean ± S.E. (n=3-4), representative of one of the two separate experiments. (D) Flowcytometry analysis of the cell surface costimulatory markers CD80, CD86, CD40, MHC Class-II expressed on splenic DCs ($CD11c^+B220^+$), 48h post-immunization, with different

DNA vaccine regimes. The data represents one of the three independent experiments (n=3) with similar results. *$p < 0.05$; **$p < 0.001$; ***$p < 0.0001$ compared to PBS controls, as assessed by one-way ANOVA and Tukey's multiple comparison test.

Figure 6.

Lower percentage of IL-4^+ and IL-10^+ T lymphocytes correlates with better vaccine outcome in *L. donovani* infected mice. Immunized BALB/c mice were challenged i.v. with 2.5×10^7 stationary phase promastigotes of *L. donovani*, ten days after booster dose. PBS-injected mice served as controls. Animals were sacrificed 3 months post-infection, followed by determination of organ weight and parasite loads in liver and spleens from the infected animals. (A) Liver and spleen weights of immunized mice 3 months post-infection. (B) Liver and spleen parasite burdens as assessed by Leishman Donovan Units (LDU) (n=4-5) of respective organs. (C) Representative micrographs (100× oil immersion) of Giemsa-stained impression smears of liver and spleen from differently immunized mice, 3 months post-infection. Arrows indicate the intracellular amastigotes. (D) Monitoring of live parasite burden per milligram of spleen and liver homogenates by limiting dilution assay (LDA) in different groups of mice, expressed as $\log_{10}$ of total organ parasite burden. Data indicate the mean ± S.E. (n=4), representative of one of the two independent experiments. *$p < 0.05$; **$p < 0.001$; ***$p < 0.0001$ compared to PBS control, as determined by one-way ANOVA and Tukey's multiple comparison test. Asterisks over line indicate significant differences between groups. Proportion of intracellular IL-12^+, IL-10^+ and IL-4^+ CD4 (E) and CD8 (F) T cells were analyzed by flowcytometry. (D) Detection of live parasite load per milligram of spleen and liver homogenates by limiting dilution assay (LDA) in the indicated groups of mice. Results are expressed as $\log_{10}$ of total organ parasite burden. Data represent mean ± S.E. (n=4), representative of one of the three independent experiments. Asterisks over line indicate

significant differences between groups. Intracellular IL-12, IL-10 and IL-4 producing $CD4^+$ (E) and $CD8^+$ (F) T cells were analysed by flowcytometry. Splenocytes from non-immunized and immunized animals were stimulated *in vitro* with 5 mg/ml rCPC, stained for surface and intracellular markers and analyzed in a LSR Fortessa flowcytometer. Single cytokine producers in each lymphocyte population are depicted from mice immunized with naked pVAX1-*cpc* and pVAX1-*cpc* entrapped in cationic liposomes with or without intrabilayer MPLA. Data represent the mean ± S.E. (n=4), as analysed by two-tailed paired Student's t test, and levels of significance are indicated by P values.

Figure 7.

Cytokine (IFN-γ, IL-12, IL-4, IL-10 and TGF-β) profile in BALB/c mice immunized with different vaccine regimes before and after *L. donovani* challenge. Ten days post-immunization and 3 months post-infection, splenocytes were collected aseptically from the different experimental animals and restimulated with rCPC (2.5μg/ml) for 72h (at 37°C, 5% CO_2). The culture supernatants were assayed for IFN-γ (A), IL-12 (B), IL-4 (C), IL-10 (D) and TGF-β (E) through ELISA as detailed in Materials and Methods. Data indicate the mean ± S.E. (n=5), representative of one of the two independent experiments. $*p < 0.05$; $**p < 0.01$; $***p < 0.001$ compared to PBS controls, as assessed by one-way ANOVA and Tukey's multiple comparison test. Ratio of secreted cytokines IFN-γ/IL-4 (F) and IFN-γ/IL-10 (G) from splenocytes of immunized and control mice were calculated upon *in vitro* stimulation with rCPC (2.5μg/ml).

Figure 8.

MPLA liposomal DNA vaccination markedly enhances the magnitude of polyfunctional, antigen-specific $CD4^+$ and $CD8^+$ T cells, induced by liposomal pVAX1-*cpc* immunization with or without intrabilayer MPLA, after *L. donovani* infection. Splenocytes isolated from immunized mice were stimulated with rCPC (2.5μg/ml), 3 months post-infection, and

analysed by multicolour flowcytometry (with Boolean gating using FlowJo software) to detect the intracellular IFN-γ, IL-2, and TNF-α produced by $CD4^+$ and $CD8^+$ T cells. (A) Representative plot showing total frequency of IFN-γ^+, IL-2^+ or TNF-α^+ $CD4^+$ T cells. (B) Frequency of $CD4^+$ T cells expressing each of the seven possible combinations of IFN-γ^+, IL-2^+ and TNF-α^+ cells. (C) The overall polyfunctionality of the $CD4^+$ T cells as visualized through pie-charts in which each slice represents the relative percentage of IFN-γ^+, IL-2^+ and TNF-α^+ categories of $CD4^+$ T cell subset within each immunized group. Phenotypic descriptions of each subset with the matching colour code are shown at bottom. (D) Representative plot showing total frequency of IFN-γ^+, IL-2^+ or TNF-α^+ $CD8^+$ T cells. (E) Frequency of $CD8^+$ T cells expressing each of the seven possible combinations of IFN-γ^+, IL-2^+ and TNF-α^+ cells. (F) The pie-chart showing the relative percentage of IFN-γ^+, IL-2^+ and TNF-α^+ $CD8^+$ T cells within each immunized group. Phenotypic descriptions of each subset with the matching colour code are shown at bottom. Values inside the boxes depict the percentage of cytokine positive cells. Data represent the mean ± S.E. (n= 3-4). SSC: Side scatter, FSC: forward scatter. Results of indicated groups were compared by two-tailed paired Student's t-test, and levels of significance are indicated by P values.

Figure 9.

Generation of appreciable CD62L and CD44 memory T cell subsets in splenocytes isolated from differently immunized mice, after *L. donovani* challenge. (A) The gating strategy used to analyse the CD62L versus CD44 on gated $CD3^+CD4^+$ and $CD3^+CD8^+$ T cells on splenocytes from different immunized groups, to determine the proportion of naive ($CD44^{low}$ $CD62L^{high}$), central memory ($CD44^{high}$ $CD62L^{high}$, T_{CM}) and effector memory ($CD44^{low}$ $CD62L^{high}$, $T_{EFF/EM}$) T cells. Lymphocytes were stained with anti-CD3-PE, anti-CD4-PerCPCy5.5, anti-CD8-APCCy7, anti-CD62L-APC and anti-CD44-FITC. Cells were first

gated onto lymphocytes and then on single cells and $CD3^+$ cells. Cells were then gated onto $CD4^+$ or $CD8^+$ cells, which were then gated further according to expression of CD44 and CD62L. The effector memory ($CD44^{high}$ $CD62L^{low}$, $T_{EFF/EM}$) T cells were further analysed for intracellular IFN-γ. The representative plots for the frequency of naive, T_{CM} and $T_{EFF/EM}$ cells within gated $CD4^+$ (B), $CD8^+$ T cells (C) and the respective summary of data in bar graphs (D & E) are shown. (F) Ag-specific intracellular IFN-γ secretion from $T_{EFF/EM}$ cells in immunized and control mice, 3 months after virulent challenge. Data represent the mean ± S.E. (n= 3-4), of two independent experiments. SSC: Side scatter, FSC: forward scatter. *$p < 0.05$; **$p < 0.01$; ***$p < 0.001$ compared to PBS controls, as assessed by one-way ANOVA and Tukey's multiple comparison test.

Table 1.

Vesicle size, zeta potential and plasmid DNA incorporation into the liposomes. Liposomal vesicles were formulated with DSPC, cholesterol, SA and MPLA at a molar ratio of 7:2:2:0.0016 either empty or loaded with the plasmid pVAX1-*cpc*, as detailed in Materials and Methods. Results represent mean ± S.E. of three independent liposome preparations. N/A- Not Applicable.

Formulation	**Vesicle size** (nm ± S.E.)	**Zeta potential** (mV ± S.E.)	**DNA encapsulation** (% total ± S.E.)
Empty liposome	151 ± 23.86	24.3 ± 3.1	N/A
Liposomes with entrapped pVAX1-*cpc*	134 ± 14.31	22.6 ± 1.2	77.7± 6.5

Liposomal vesicles were formulated with DSPC, cholesterol, SA and MPLA at a molar ratio of 7:2:2:0.0016 either empty or loaded with pVAX1-*cpc*, as described in Materials and Methods. Results represent mean ± S.E. two independent experiments. N/A- Not applicable.

Supporting Information

1. Materials and Methods

1.1 Cloning and purification of recombinant *L. donovani* CPC and production of polyclonal antiserum.

1.2. MTT Assay

1.3. Tranfection of HEK-293T cells with pVAX1-*cpc*.

1.4. BMDC culture and western blot.

2. Supplementary table

Table S1. Ag-specific IgG isotype profiles in mice differently immunized with before and after *L. donovani* challenge.

3. Supplementary figures

Figure S1.

Transfection efficacy of the cationic DSPC-MPLA liposomes in RAW264.7 cell line.

Figure S2.

Uptake efficacy of MPLA- liposomes in different cell lines.

Figure S3.

Gating scheme for identification of polyfunctional T-cells.

Figure S4.

Giemsa-stained impression smears of livers and spleens from differently immunized mice.

Figure S5.

DTH response in mice immunized with different pVAX1-*cpc* immunization regimens, after 3 months post-challenge.

Figure S6.

Analysis of liposomal entry into the draining lymph nodes (dLNs) using flowcytometry.

Figure S7.

PCR analysis for biodistribution of pVAX1-*cpc* in different tissues of BALB/b mouse, 48 h post immunization via i.m. route.

FIGURE 1

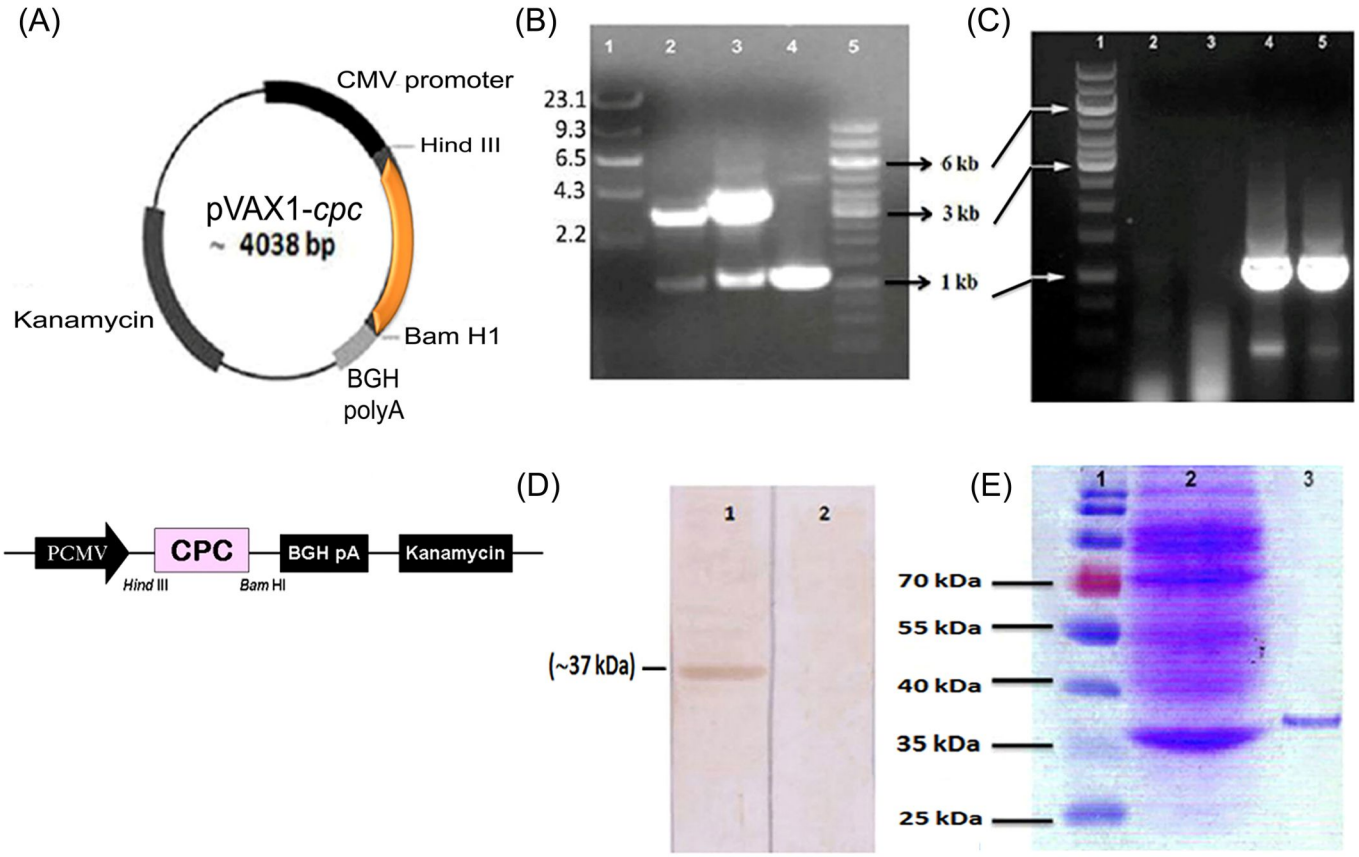
(A)
CMV promoter
Hind III
pVAX1-cpc
~ 4038 bp
Kanamycin
Bam H1
BGH
polyA
PCMV
CPC
BGH pA
Kanamycin
Hind III
Bam HI
(B)
1 2 3 4 5
23.1
9.3
6.5
4.3
2.2
6 kb
3 kb
1 kb
(C)
1 2 3 4 5
(D)
1 2
(~37 kDa)
(E)
1 2 3
70 kDa
55 kDa
40 kDa
35 kDa
25 kDa

FIGURE 2

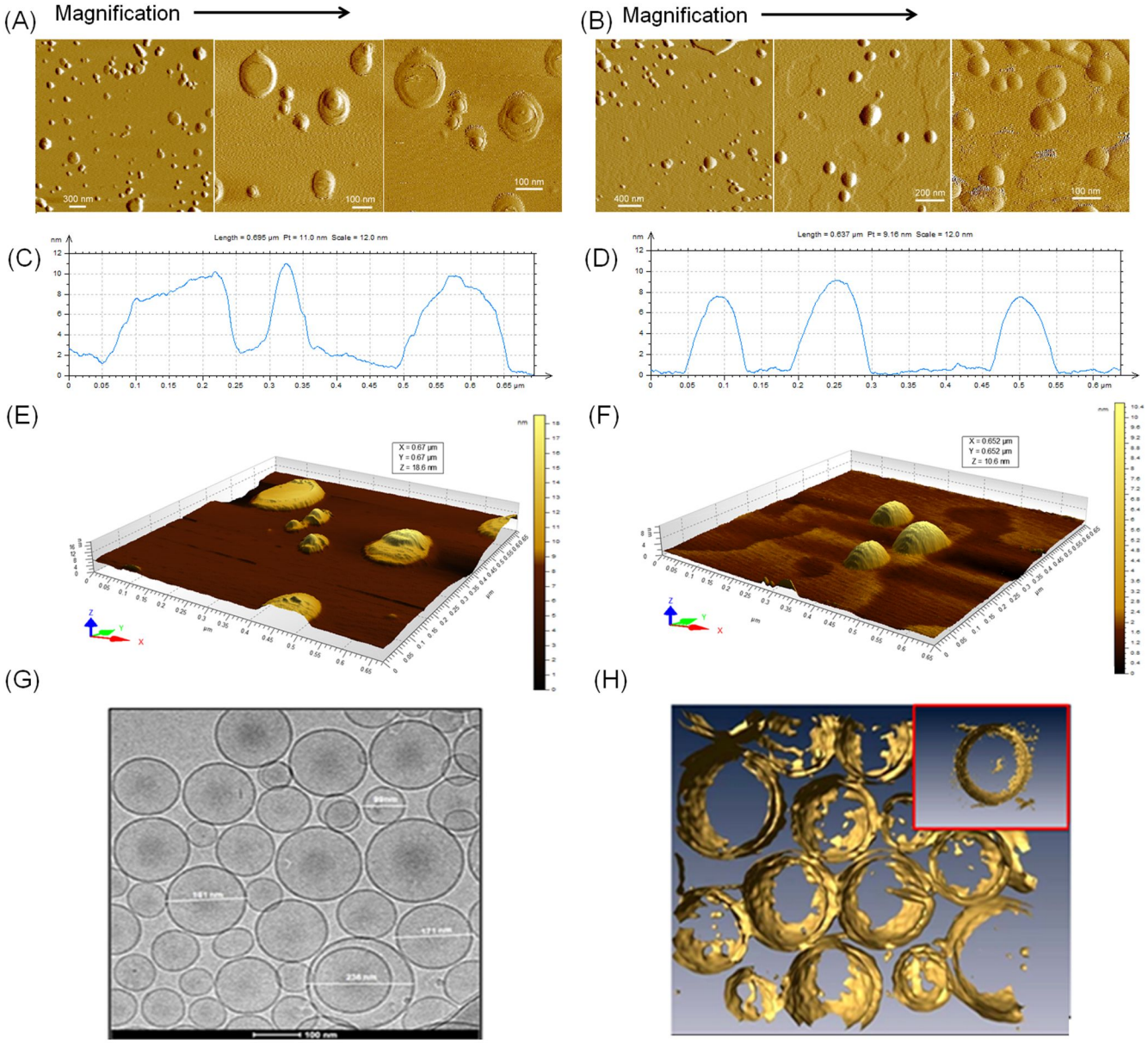
(A)
Magnification
300 nm
100 nm
100 nm
(B)
Magnification
400 nm
200 nm
100 nm
(C)
Length = 0.695 µm Pt = 11.0 nm Scale = 12.0 nm
(D)
Length = 0.637 µm Pt = 9.16 nm Scale = 12.0 nm
(E)
X = 0.67 µm
Y = 0.67 µm
Z = 18.6 nm
(F)
X = 0.652 µm
Y = 0.652 µm
Z = 10.6 nm
(G)
(H)

FIGURE 3

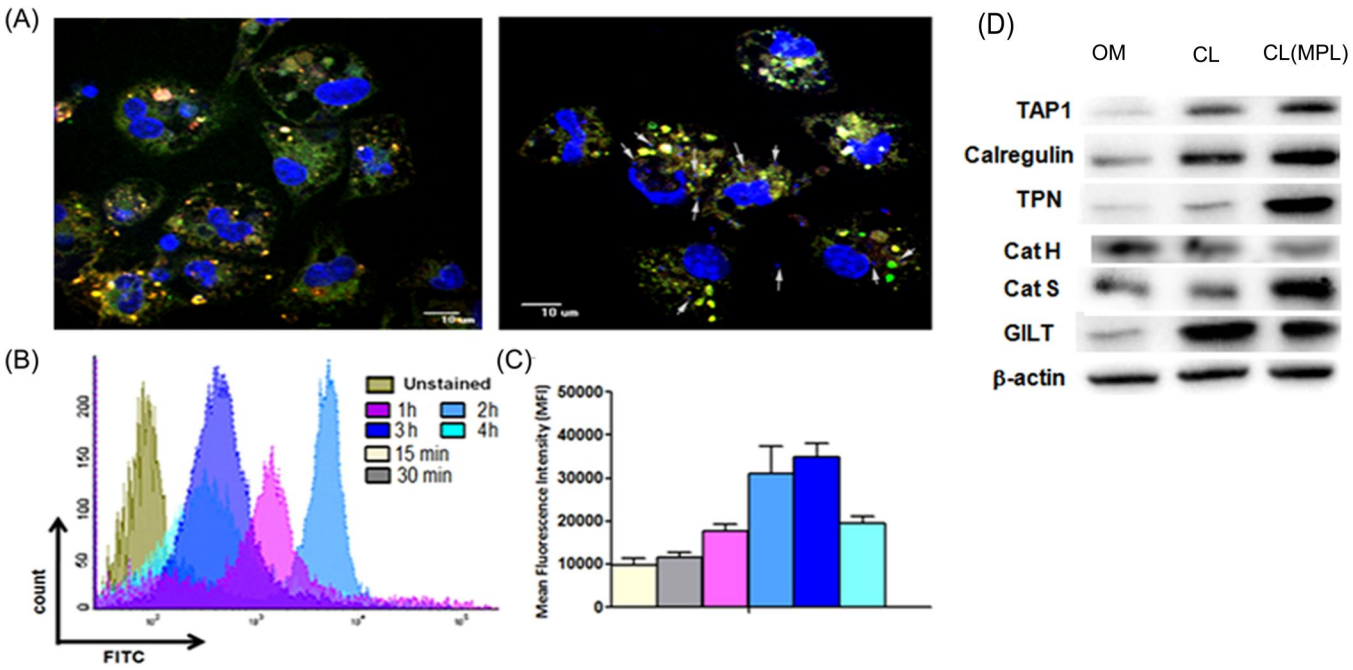
(A)
10 um
(B)
Unstained
1h
2h
3h
4h
15 min
30 min
count
FITC
(C)
Mean Fluorescence Intensity (MFI)
50000
40000
30000
20000
10000
0
(D)
OM
CL
CL(MPL)
TAP1
Calregulin
TPN
Cat H
Cat S
GILT
β-actin

FIGURE 4

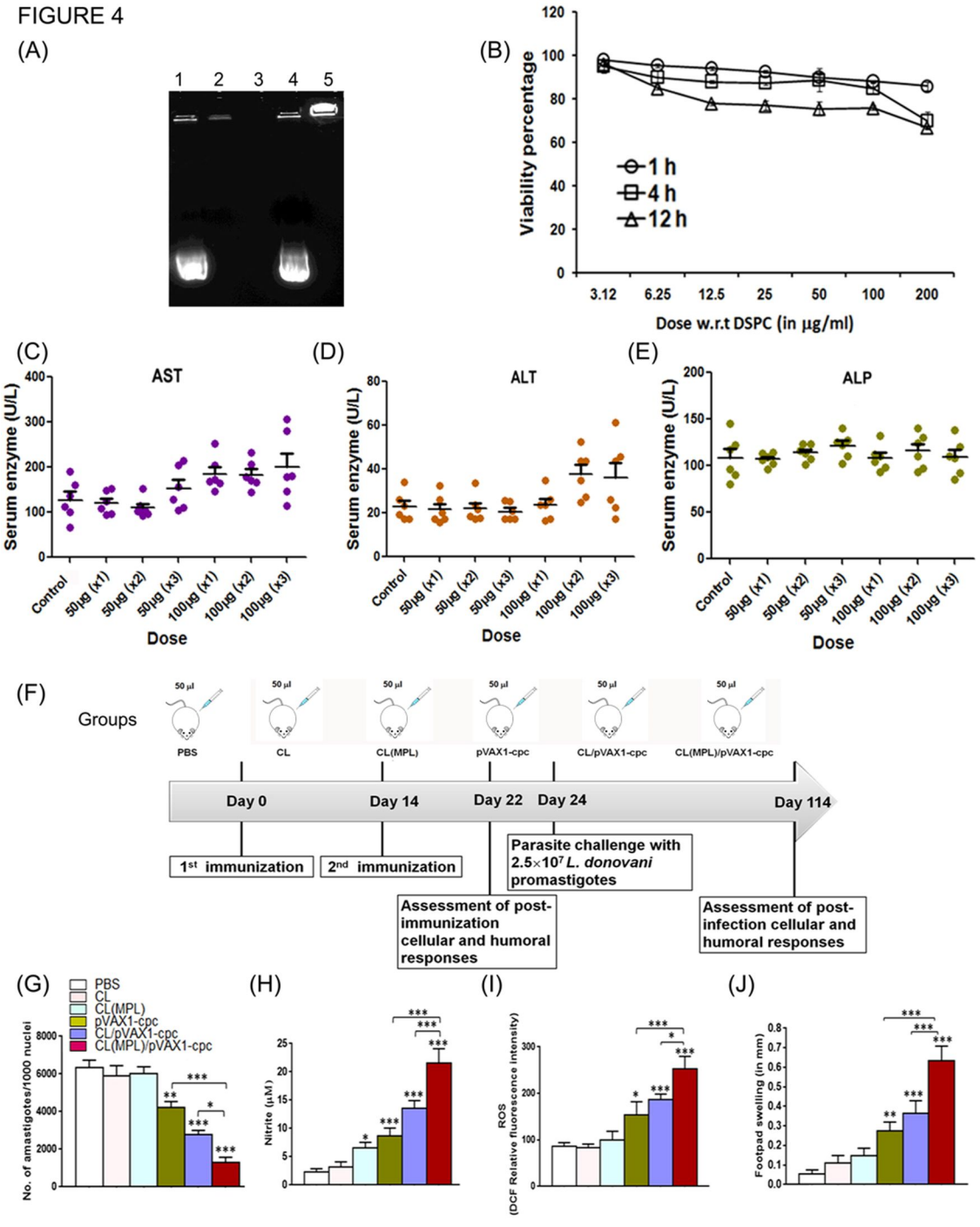
(A)
1 2 3 4 5
(B)
Viability percentage
1 h
4 h
12 h
Dose w.r.t DSPC (in µg/ml)
(C)
AST
Serum enzyme (U/L)
Control
50µg (x1)
50µg (x2)
50µg (x3)
100µg (x1)
100µg (x2)
100µg (x3)
Dose
(D)
ALT
Serum enzyme (U/L)
Dose
(E)
ALP
Serum enzyme (U/L)
Dose
(F)
Groups
PBS
CL
CL(MPL)
pVAX1-cpc
CL/pVAX1-cpc
CL(MPL)/pVAX1-cpc
Day 0
Day 14
Day 22
Day 24
Day 114
1st immunization
2nd immunization
Parasite challenge with 2.5×10^7 L. donovani promastigotes
Assessment of post-immunization cellular and humoral responses
Assessment of post-infection cellular and humoral responses
(G)
No. of amastigotes/1000 nuclei
(H)
Nitrite (µM)
(I)
ROS
(DCF Relative fluorescence Intensity)
(J)
Footpad swelling (in mm)

FIGURE 5

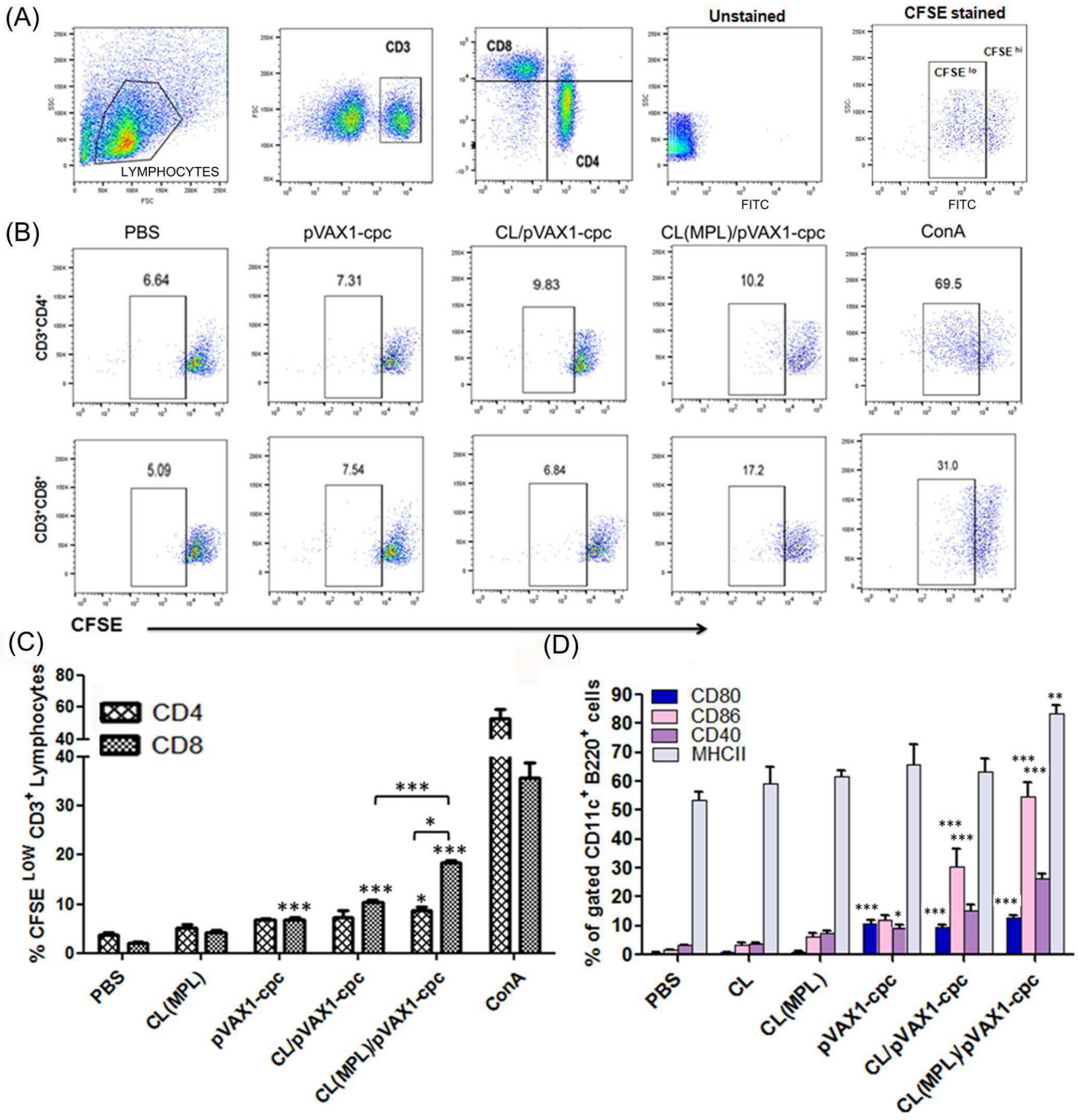
(A)
LYMPHOCYTES
CD3
CD8
CD4
Unstained
CFSE stained
CFSE hi
CFSE lo
FITC
(B)
PBS
pVAX1-cpc
CL/pVAX1-cpc
CL(MPL)/pVAX1-cpc
ConA
CD3+CD4+
6.64
7.31
9.83
10.2
69.5
CD3+CD8+
5.09
7.54
6.84
17.2
31.0
CFSE
(C)
% CFSE LOW CD3+ Lymphocytes
CD4
CD8
PBS
CL(MPL)
pVAX1-cpc
CL/pVAX1-cpc
CL(MPL)/pVAX1-cpc
ConA
(D)
% of gated CD11c+ B220+ cells
CD80
CD86
CD40
MHCII
PBS
CL
CL(MPL)
pVAX1-cpc
CL/pVAX1-cpc
CL(MPL)/pVAX1-cpc

FIGURE 6

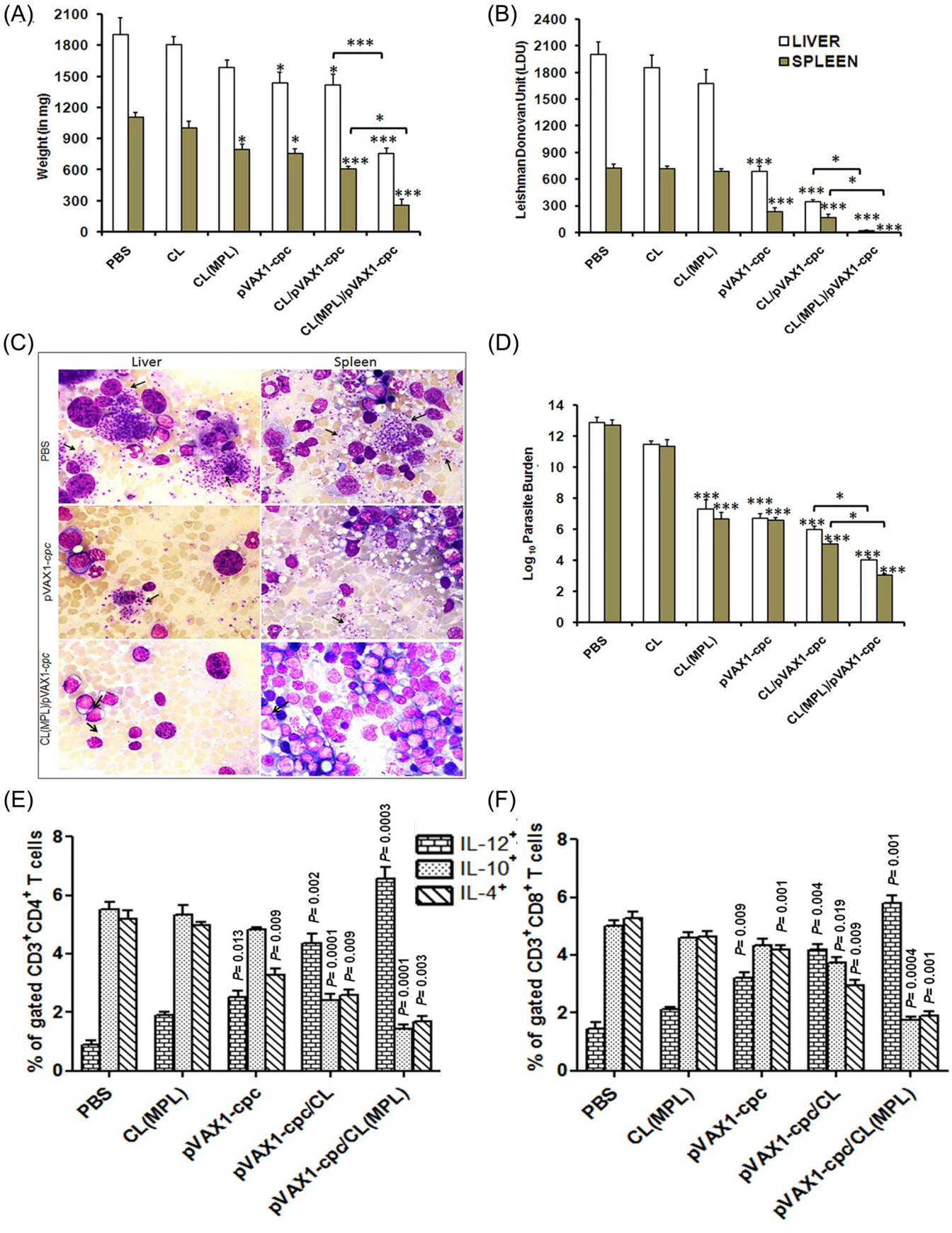
(A)
Weight (in mg)
2100
1800
1500
1200
900
600
300
0
PBS
CL
CL(MPL)
pVAX1-cpc
CL/pVAX1-cpc
CL(MPL)/pVAX1-cpc
(B)
LIVER
SPLEEN
Leishman Donovan Unit (LDU)
2400
2100
1800
1500
1200
900
600
300
0
(C)
Liver
Spleen
PBS
pVAX1-cpc
CL(MPL)/pVAX1-cpc
(D)
Log10 Parasite Burden
14
12
10
8
6
4
2
0
(E)
% of gated CD3+CD4+ T cells
IL-12+
IL-10+
IL-4+
P= 0.013
P= 0.009
P= 0.002
P= 0.0001
P= 0.009
P= 0.0003
P= 0.0001
P= 0.003
(F)
% of gated CD3+CD8+ T cells
P= 0.009
P= 0.001
P= 0.004
P= 0.019
P= 0.009
P= 0.001
P= 0.0004
P= 0.001

FIGURE 7

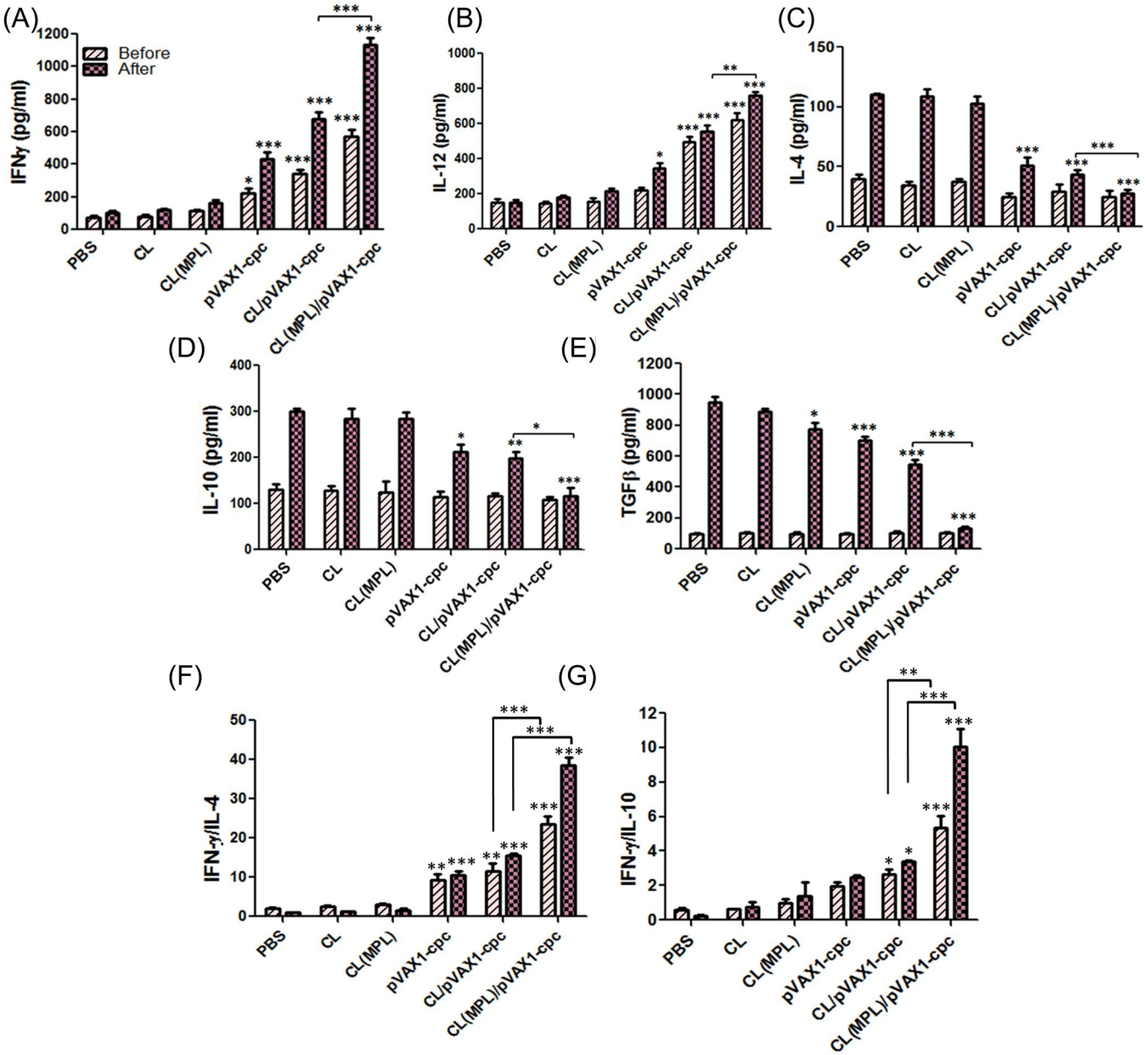
(A)
IFNγ (pg/ml)
Before
After
(B)
IL-12 (pg/ml)
(C)
IL-4 (pg/ml)
(D)
IL-10 (pg/ml)
(E)
TGFβ (pg/ml)
(F)
IFN-γ/IL-4
(G)
IFN-γ/IL-10
PBS
CL
CL(MPL)
pVAX1-cpc
CL/pVAX1-cpc
CL(MPL)/pVAX1-cpc

FIGURE8

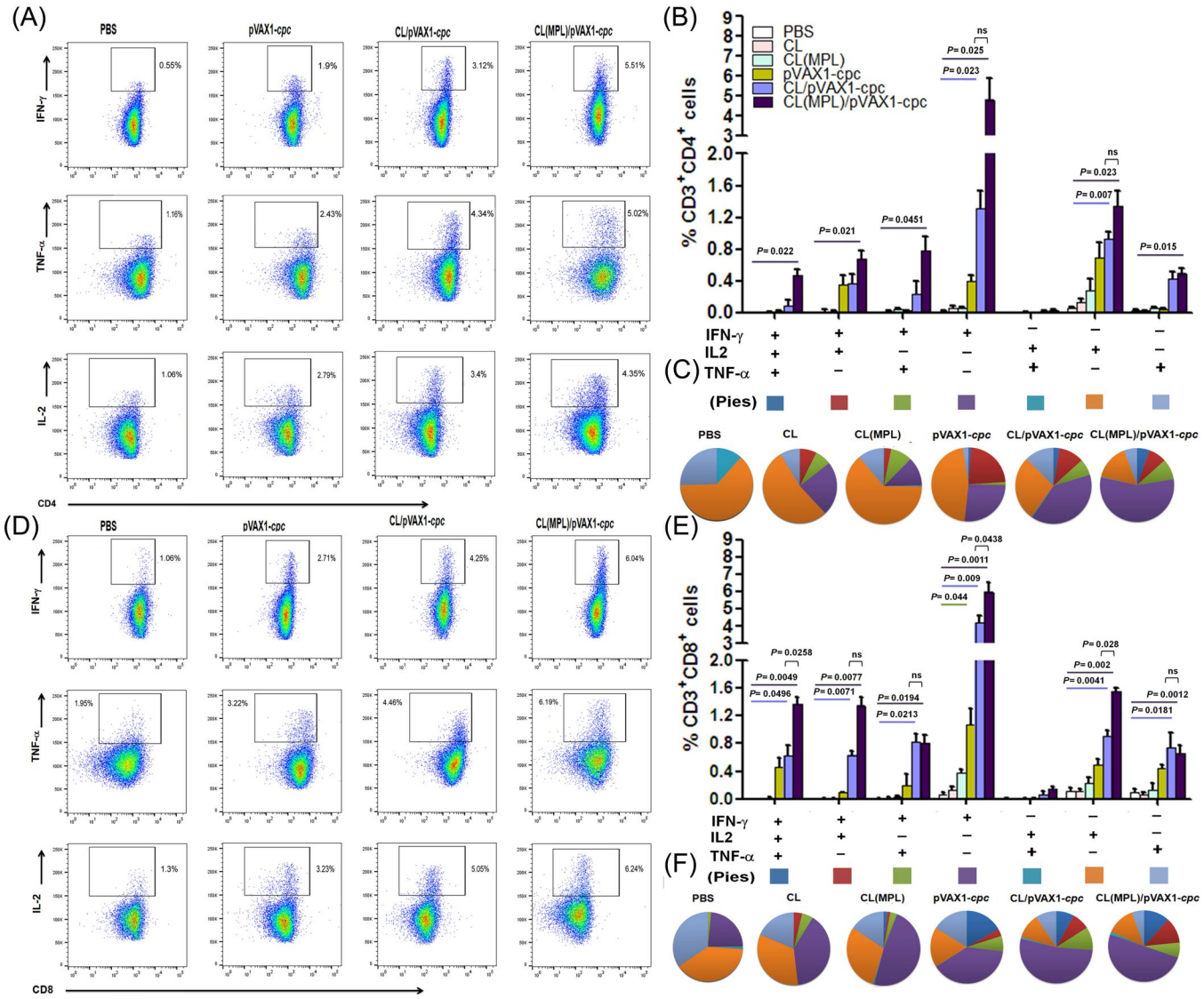
(A)
PBS
pVAX1-cpc
CL/pVAX1-cpc
CL(MPL)/pVAX1-cpc
IFN-γ
TNF-α
IL-2
CD4
0.55%
1.9%
3.12%
5.51%
1.16%
2.43%
4.34%
5.02%
1.06%
2.79%
3.4%
4.35%
(B)
PBS
CL
CL(MPL)
pVAX1-cpc
CL/pVAX1-cpc
CL(MPL)/pVAX1-cpc
% CD3+CD4+ cells
P= 0.022
P= 0.021
P= 0.0451
P= 0.025
P= 0.023
P= 0.007
P= 0.023
P= 0.015
ns
IFN-γ
IL2
TNF-α
(C)
(Pies)
PBS
CL
CL(MPL)
pVAX1-cpc
CL/pVAX1-cpc
CL(MPL)/pVAX1-cpc
(D)
PBS
pVAX1-cpc
CL/pVAX1-cpc
CL(MPL)/pVAX1-cpc
IFN-γ
TNF-α
IL-2
CD8
1.06%
2.71%
4.25%
6.04%
1.95%
3.22%
4.46%
6.19%
1.3%
3.23%
5.05%
6.24%
(E)
% CD3+CD8+ cells
P= 0.0438
P= 0.0011
P= 0.009
P= 0.044
P= 0.0258
P= 0.0049
P= 0.0496
P= 0.0077
P= 0.0071
P= 0.0194
P= 0.0213
P= 0.028
P= 0.002
P= 0.0041
P= 0.0012
P= 0.0181
ns
IFN-γ
IL2
TNF-α
(F)
(Pies)
PBS
CL
CL(MPL)
pVAX1-cpc
CL/pVAX1-cpc
CL(MPL)/pVAX1-cpc

FIGURE 9